# Estimation of Functional and Structural Parameters in the Chemical Transmission Process at the Neuromuscular Junction

March 1993

Takashi Yoda

# Estimation of Functional and Structural Parameters in the Chemical Transmission Process at the Neuromuscular Junction

Takashi Naka

Dissertation submitted to
the Doctoral Program in Engineering
University of Tsukuba Graduate School

March 1998

## Abstract

A compartment model representing the chemical transmission process of acetylcholine (ACh) at the neuromuscular junction for generation of the miniature endplate current (MEPC) is constructed as a reaction-diffusion system (RD system) in a two-dimensional space of axis-symmetrical disc of the synaptic cleft. The model is defined as the standard to have the critical radius of 500nm and the respective compartment numbers of 3 and 10 on the transverse and radial coordinates. Besides the transverse and radial diffusion processes, the model can include the release mechanism of ACh as the release rate and the release area of ACh, and the junctional fold as a concentric cylinder attached to the disc at the postsynaptic membrane. The model might be regarded as the two-dimensional extension of the similar models proposed previously, which essentially behave as one-dimensional compartment models because the diffusion process in either of two directions is simplified.

This two-dimensional compartment model is effectively applied to analysis of the functional and structural correlations in the transmission process. The simulation analysis with the model demonstrates that the diffusion coefficient for isotropic diffusion in the disc is evaluated to be $1.0 \times 10^{-6}\mathrm{cm}^2\mathrm{sec}^{-1}$, with which the model reproduces the behavior of the MEPC from the empirical analysis with respect to the characteristic parameters. It further follows that in the RD system with anisotropic diffusion the radial diffusion has more distinctive effects on the MEPC than the transverse diffusion. The neurotransmitter release mechanisms of the expanding pore and the acceleration release are examined to reveal that the expanding rate more than 10nm/msec and the acceleration rate 10 times of the natural diffusion with the diffusion coefficient around $1.0\times10^{-6}\mathrm{cm}^2\mathrm{sec}^{-1}$ could reproduce the empirical MEPC. The effects of the junctional fold and the synaptic vesicle are further analyzed to elucidate their unknown functions associated with the specific structures at the neuromuscular junction. The width of the junctional fold has more distinctive effects than the depth in enlargement of the reacting area of the postsynaptic membrane. The quantal release mechanism raises significantly the amplitudes of MEPC and the endplate current (EPC). The localized release of ACh has the similar effect on EPC compared with the homogeneous release of ACh.

# Contents

# List of Figures

# List of Tables

# Chapter 1

# Introduction

Intensive studies of the relationships between the structures and functions of living systems in biochemistry and molecular biology have revealed that the biological functions all stem from biochemical reactions within the systems such as cells, tissues, organs, and individual organisms. On processing of the neuronal signals, investigation of the molecular events in the synaptic chemical transmission has led to the neurotransmitter theory [17]. The best understood chemical synapse with a typical neurotransmitter is that called neuromuscular junction at which acetylcholine (ACh) is engaged in the chemical transmission between a motor neuron and muscle cells.

An action potential arrives at the end of the motor neuron in nerve fiber, and depolarizes the synaptic terminal to induce the quantal release of ACh stored inside the terminal. It is now widely accepted that a quantum of ACh is released by exocytosis, that is, the fusion of a synaptic vesicle with the presynaptic membrane. The ACh molecules released diffuse in the synaptic cleft, undergoing hydrolysis by acetylcholinesterase (AChE), and then bind with ACh receptor (AChR) to alter the ionic permeability of the muscle cell membrane, producing depolarization of the muscle cell membrane to cause the contraction of the muscle cells. Presumably, AChEs are homogeneously distributed in the synaptic cleft and AChRs are concentrated on the postsynaptic membrane.

The depolarization of the muscle cell membrane has been measured as the current through the membrane called endplate current (EPC) or miniature endplate current (MEPC) which is the EPC responding to a quantal release of ACh. The MEPCs are observed as the spontaneous generation under the normal physiological condition, which occurs due to occasional

and small depolarization without any presynaptic action potential. The generation of MEPC at the neuromuscular junction has been studied as an elementary process of the chemical transmission process and a lot of empirical data have been accumulated. In this study a model representing the elementary process is proposed on the basis of these empirical data, and applied to reveal some of the functional and structural correlations in the chemical transmission process employing the computer simulation method [10, 16].

The dynamic behavior of neurotransmitter in the processes of diffusion through the synaptic cleft and action at the synaptic membranes is associated with a fundamental function for the chemical transmission process. Analysis of such behavior can be performed most appropriately with representation of the transmission process as a reaction-diffusion system (RD system) for neurotransmitter because the experimental analysis still is practically difficult for the molecular processes in the synaptic cleft. Some mathematical models have been proposed for the dynamic behavior of ACh in generation of the MEPC at the neuromuscular junction. In the RD system representing the transient process of ACh at the neuromuscular junction, the ACh concentration varies with time and position in the space of the synaptic cleft, due to transverse and radial diffusion of ACh and its interaction with AChR and AChE. In the model of Rosenberry [26] the radial diffusion process of ACh is simplified as the two axis-symmetrical compartments with homogeneity assumed in the transverse direction. Wathey *et al.* [32] extended the model to a one-dimensional compartment model in the radial direction by discretization of the radial coordinate of the RD system. In the model of Friboulet *et al.* [7] the transverse coordinate is discretized and the radial diffusion undergoes simple efflux of ACh due to concentration gradient.

The behavior of the RD system of ACh responsible for generation of the MEPC is mathematically expressed by a two-dimensional diffusion equation with nonlinear reaction terms for ACh and a set of nonlinear ordinary differential equations governing the rate processes for AChR and AChE. The analysis of temporal behavior of the RD system employs the computer simulation, that is, numerical integration of partial differential equation by means of discretization of both the transverse and radial coordinates in the space, which results in a two-dimensional compartment model for full representation of both of the transverse and

radial diffusion processes of ACh. It thus follows that the one-dimensional compartment models previously proposed are regarded as the special cases of the two-dimensional compartment model with either of the transverse or radial diffusion process embedded in one compartment. The validity of the reduction of dimension may depend on the phenomenon to be analyzed, and is examined in this study by determination of the appropriate number of the compartments for the two-dimensional compartment model.

With the compartment numbers determined, the model is applied to analyze the dynamic behavior of ACh in the synaptic cleft in generation of the MEPC responding to a quantal release of ACh at the neuromuscular junction. The effect of the diffusion coefficient of ACh in the cleft and the release mechanism of ACh from the synaptic vesicle are chosen to be analyzed for characterization of the mechanisms in the chemical transmission process because the experimental analysis is still difficult on these problems. The effects of the specific structures at the neuromuscular junction such as the junctional fold and the synaptic vesicles are also analyzed to elucidate their unknown functions.

The contents in the chapters of this dissertation are summarized as follows. In Chapter 2 the structures of the synaptic region and the mechanism of generation of the MEPC at the neuromuscular junction are described on the basis of reported observations with electron microscope technique and various experimental studies. The neuromuscular junction has a structural feature of superficial gutters called junctional folds aligned at regular intervals on the muscle fiber. Mathematical models of the RD system which have been proposed to reveal some features are also described. The models are classified into two categories by simulation methods, that is, Monte Carlo method and differential equation method. The models previously proposed in the class of differential equation method may be derived as the special cases of the compartment model constructed in this study.

In Chapter 3 a compartment model in a two-dimensional space of axis-symmetrical disc is constructed for analysis of the chemical transmission processes of ACh in the synaptic cleft at the neuromuscular junction. The behavior of the RD system is expressed by a two-dimensional diffusion equation with nonlinear reaction terms due to the rate processes with AChR and AChE. The method of lines is then applied to discretize the partial differential

equation with respect to the space variables, resulting in a set of nonlinear ordinary differential equations called a compartment model with spacial compartments in the disc. Numerical integration of the system of ordinary differential equations by the Gear method now yields the temporal behavior of ACh in the RD system. The validity of the reduction of dimension is also examined in considering the appropriate number of the compartments.

In Chapter 4 the compartment model is applied for characterization of the mechanisms in the chemical transmission process by the computer simulation of the RD system. The dynamic behavior of the RD system is characterized with its parameters such as kinetic parameters for the reactions in the cleft and the release mechanism of ACh, diffusion coefficient of ACh in the cleft, and structural parameters of the synaptic cleft. In this study the diffusion coefficient of ACh and the release mechanisms are examined for the effects on generation of the MEPC at the neuromuscular junction. The simulations are performed with the various values of these parameters for quantitative characterization of the dynamic behavior of the RD system, estimating the suitable values of the parameters with respect to reproduction of the empirical MEPC.

Another aspect of application of the compartment model is demonstrated in Chapter 5. The biochemical systems have been developed through the long lasting evolution process, implying that sorts of quantitative optimization might have been accomplished with respect to the parameters associated with the functions of the systems. Hence, the parameters in the chemical transmission process would be optimal with respect to the generation of MEPC. The structural parameters, such as the width and depth of the junctional folds and the localization of the release area of ACh due to the structure of the synaptic vesicles, are examined with regard to the generation of MEPC to lead to elucidation of the significance of the specific structure of the neuromuscular junction and the quantal release of neurotransmitter. The evaluation of the size of the release area is further attempted with regard to the EPC responding to arrival of the action potential at the nerve terminal.

# Chapter 2

# Mechanisms for Chemical Transmission Process

Much effort has been made on the purpose of elucidation at the molecular level of the relationships between structures and functions of neurons and synapses. There exist two general classes of synapses: the electrical and chemical synapses. The neuromuscular junctions (sometimes also called the myoneural junction) are the best clarified chemical synapses with which the motor nerve terminal connects to the muscle fiber. In this chapter the structures of the neuromuscular junction and the chemical transmission mechanism for generation of the MEPC are described to summarize the reported observations with electron microscope technique and various experimental studies.

At the neuromuscular junction the motor nerve terminal lies in a shallow "gutter", that is, depressions formed on the muscle fiber where the superficial gutters are aligned at regular intervals called junctional folds. The synaptic terminal contains a large number of tiny, membrane-bound structures called synaptic vesicles which are filled with the neurotransmitter of ACh. The chemical transmission process is comprised of three basic processes for ACh: release from the presynaptic membrane, diffusion and hydrolysis by AChE in the synaptic cleft, and interaction with AChR for the EPC generation at the postsynaptic membrane. On arrival at the end of the motor neuron nerve fiber, an action potential depolarizes the synaptic terminal, and induces the quantal releases of ACh stored inside the synaptic vesicles with their fusion to the presynaptic membrane. The ACh molecules released diffuse in the synaptic cleft, and bind with AChE for hydrolysis and with AChR to alter the ionic permeability of the muscle cell membrane, resulting in depolarization of the membrane and

contraction of the muscle cells. The generation of MEPC works as an elementary process of the chemical transmission process.

This chapter is concluded to describe some mathematical models which have been proposed to analyze the transient process of the synaptic chemical transmission by representing the dynamic behavior of ACh in generation of the MEPC at the neuromuscular junction. The models are classified into two categories by simulation methods, that is, Monte Carlo method and differential equation method. The practical limitations of computational costs are much different in the two methods, depending on the complexity of the problem to be solved. The models by the differential equation method are further classified with respect to the dimension of the space in which ACh diffuses. The compartment model proposed in this study is a model by the differential equation method in a two-dimensional space of the synaptic cleft. The models described in this chapter may be derived as the special cases of this compartment model.

## 2.1 Structures of the neuromuscular junction

One of the well-known neuromuscular junctions is associated with "fast" skeletal muscle fibers in the frog, where the myelinated motor axon approaches to the muscle fiber, and gives off an array of non-myelinated terminal branches which spread along the fiber surface in both directions. The terminal branch runs parallel to the axis of the muscle fiber, and lies in a shallow "gutter", that is, depression formed on the fiber surface. Figure 2.1(a) shows a diagram of a small part of a terminal branch facing the muscle cell with an additional structure called junctional folds which form the superficial gutters in regular intervals at a right angle to the fiber axis with openings to the external space at both sides of the nerve terminal. The longitudinal spacing of the folds is rather regular: approximately 3 to 4 per sarcomere, while the width of the fold varies between about 50nm and well over 100nm [5].

The schematic view of the longitudinal section of a terminal branch in Fig. 2.1(b) illustrates that the pre- and post-synaptic membranes are juxtaposed closely to form the synaptic cleft of about 50nm [24]. The region of muscle membrane for the synaptic contact is called the endplate region, which possesses the special characteristics. In particular, the endplate membrane is rich in a trans-membrane protein of AChR as indicated by thick line in Fig. 2.1(b). The receptor acts as an ionic channel which opens when it binds with ACh. In the frog muscle AChR is localized on the postsynaptic membrane and approximately the top 50% of the junctional folds, and the receptor site density is about $26,000 \pm 6000$ sites/$\mu$m$^2$, which falls sharply to about 50 sites/$\mu$m$^2$ within 15$\mu$m from the synaptic region [19]. On the other hand, the AChE activity appears to be not only on the pre- and post-synaptic membranes but also homogeneously in all the space in the synaptic cleft [6].

The synaptic terminal contains a large number of tiny, membrane-bound structures called synaptic vesicles which are filled with ACh molecules. The diameter of the vesicle is of the order of 50nm [5]. It is natural to assume that the vesicles represent the packets of ACh which are released in response to an action potential. Indeed, it is observed that these vesicles are depleted by any manipulation causing release of large amount of ACh, such as prolonged depolarization or firing of large numbers of action potentials. It is now generally accepted that ACh is released by the fusion of the vesicle membrane with the plasma membrane of the

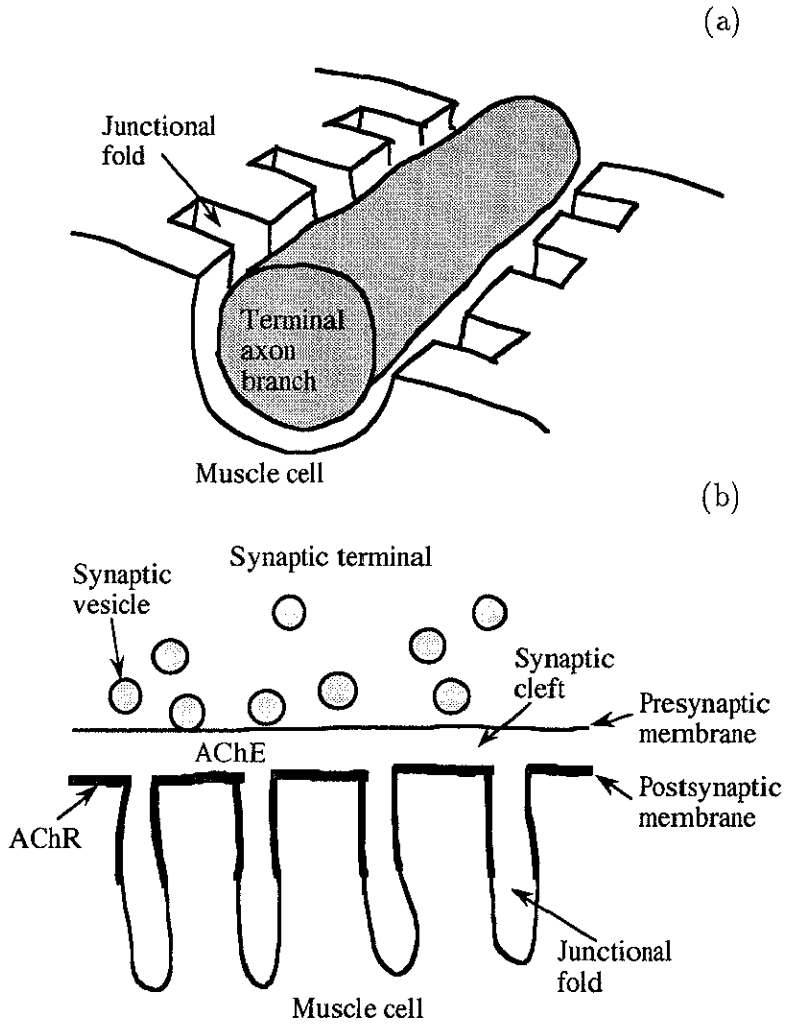


**Fig.2.1.** Structures of a neuromuscular junction. (a) Diagram of a small part of the terminal branch at a neuromuscular junction. (b) Schematic longitudial-sectional view of the neuromuscular junction with some characteristic components.

synaptic terminal, dumping the content of the vesicle into the synaptic cleft. The vesicles fuse only at specific membrane regions called release sites or active zones. The active zone of the presynaptic terminal appears in the freeze-fracture electron microscopy as a double row of large membrane particles which are probably membrane proteins involved in the fusion [17].

## 2.2 Generation of miniature endplate current

### 1. Release of chemical transmitters

The fact that the quanta consisting of many molecules of ACh are released from the motor nerve terminal implies that the basic unit of release is not a single molecule of ACh but the quantum. At the neuromuscular junction, it is estimated that a single quantum contains about 10,000 molecules of ACh and a single action potential normally causes the release of more than a hundred quanta from the synaptic terminal [17].

It is now widely accepted that a quantum of ACh is released by the fusion of a synaptic vesicle with the presynaptic membrane, which is called exocytosis [18, 31]. During the early stages of exocytosis, vesicles in neurons and other secretory cells appear to be connected to the extracellular space by narrow pores but the details of the mechanism of the fusion process are unknown. For the study of the release mechanism the empirical data obtained from secretory vesicles in the mast cells have been used since the biophysical mechanisms underlying membrane fusion and pore expansion for synaptic vesicles and secretory granules have common features. Measurement of the conductance of the fusion pore of the mast cell infers that the pore must have molecular dimensions, that is, its length and diameter are to be 10-15nm (thickness of two membranes) and about 2nm, respectively and the diameter increases with the median rate of 0.8nm/ms after the pore opens, with the assumption of cylindrical form of the pore [28].

A recent study of the ACh release mechanism with the parameters of the mast cell mentioned above suggests that the growth time of the MEPC is too long to agree with the time course empirically known and those generated by the previous models with the instantaneous spread of ACh assumed [12]. The study also described the possibility of the active release mechanism coupled with the ion exchange to explain the empirical data. It is further proposed as another possibility to justify the empirical data that ACh molecules would be released through the pore expanding rapidly with the rate of about 25nm/ms which is much faster than that of the mast cell [29]. On the other hand, Van der Kloot [30] has a doubt in the empirical data for the mean growth time from 20% to 80% of the MEPC to be too short, and reports 250$\mu$s as the growth time of the MEPC obtained from the new

measurement procedure instead of 100$\mu$s used in the previous studies.

## 2. Diffusion and reactions in the synaptic cleft

The ACh molecules released from the synaptic terminal diffuse across the synaptic cleft with simultaneous undergoing of the hydrolysis by AChE, and then reach the AChR-distributed postsynaptic membrane where AChE and AChR compete for binding with ACh. On double binding with ACh the functionally dimeric AChR transforms between the open and closed channel forms so that opening of the channel leads to generation of the MEPC. In the cleft AChE rapidly hydrolyzes ACh into choline (Ch) and acetate, which are then taken up into the nerve terminal for use in the metabolic loops.

The diffusion process of ACh is formulated by Fick's second law as follows:

$$\frac{\partial A}{\partial t} = D\nabla^2 A \tag{2.1}$$

where $A$ denotes the concentration of ACh at a position in the cleft and at time $t$, and the coefficient $D$ is called the diffusion coefficient. The value of $D$ for ACh is estimated to be 9.8 (s.e.$\pm$0.42) $\times 10^{-6}$cm$^2$sec$^{-1}$ at 20 $\pm$ 1°C in agar gels, and in the rat diaphragm the value is only 1/7 of that expected from diffusion in agar gel [13]. However, the accurate value of the diffusion coefficient of ACh in the milieu of the synaptic cleft is still unknown. As experimental measurement of the diffusion coefficient of ACh in the cleft is virtually impossible at present, the value has been evaluated through the mathematical models with the other empirical data. It is reported that the value of about $8 \times 10^{-7}$cm$^2$sec$^{-1}$ causing 10 times slower than free diffusion [19] and a higher value of $4 \times 10^{-6}$cm$^2$sec$^{-1}$ [14, 15] are predicted by kinetic simulation models, and the value of $2 \times 10^{-6}$cm$^2$sec$^{-1}$ is calculated [20] from the data of electrophysiological observations [11].

The interaction of ACh with functionally dimeric AChR follows the minimal mechanism [7, 14] as given in:

$$\mathrm{ACh} + \mathrm{R} \underset{k_{-r}}{\overset{2k_r}{\rightleftharpoons}} \mathrm{R}_1 \qquad \mathrm{ACh} + \mathrm{R}_1 \underset{2k_{-r}}{\overset{k_r}{\rightleftharpoons}} \mathrm{R}_2 \underset{k_c}{\overset{k_o}{\rightleftharpoons}} \mathrm{R}_o \tag{2.2}$$

where R and $\mathrm{R}_1$ indicate the AChR species free and singly bound with ACh, respectively. The $\mathrm{R}_2$ is an AChR species doubly bound with ACh for the closed channel form, which

interconverts to the open channel form $R_o$. The $k_i$'s ($i = r, -r, o, c$) are the rate constants for the respective steps in the mechanism. It is assumed in this study that the time course of the total number of the open channel form of AChR (i.e., $R_o$) represents the transient evolution of the MEPC. The desensitization of AChR with ACh is not included in the minimal mechanism because it evolves much more slowly than the generation of MEPC and the hydrolysis of ACh by the AChE reaction.

The reaction of AChE proceeds in the following mechanism originally proposed by Rosenberry [25]:

$$\mathrm{ACh} + \mathrm{E} \underset{k_{-1}}{\overset{k_1}{\rightleftharpoons}} \mathrm{X_1} \overset{k_2}{\rightarrow} \mathrm{X_2} + \mathrm{Ch} \qquad \mathrm{X_2} \overset{k_3}{\rightarrow} \mathrm{E} + \mathrm{acetate} \tag{2.3}$$

where E, $X_1$ and $X_2$ denote the AChE species free, complexed with ACh and acetyl group, respectively. The $k_i$'s ($i = 1, -1, 2, 3$) are the rate constants for the respective steps in the mechanism.

The behavior of the MEPC responding to the quantal release of ACh may be characterized quantitatively with the amplitude (maximum value of MEPC), growth time (time to increase from 20% to 80% of the amplitude) and decay constant (time constant for exponential decay of MEPC). It is known from the experimental analysis of the typical MEPC [26] that the amplitude is about 10% of the total number of ACh molecules released, either in the frog or rat junctions. The growth time is quite variable but the average value is about $120\mu$sec in frog as well as in eel electroplax. The decay phase is very sensitive to both temperature and the postsynaptic membrane voltage. The average value of the decay constant is 1.7msec in frog and 0.6msec in eel electroplax. With AChE inhibition, relative amplitude for MEPC increases about 1.5- to 2-fold in the frog junctions; the growth time shows little increase, and the decay phase is prolonged two- to four-fold. It is also reported that the number of the open channel form of AChR at the peak of MEPC is 1500 [7] and the mean growth time is about $250\mu$sec for frog [30].

## 2.3 Mathematical models of the chemical transmission process

### 1. Overview

Analysis of the dynamic behavior of neurotransmitter in diffusion and reactions in the synaptic cleft can be performed most appropriately with representation of the transmission process as a reaction-diffusion system (RD system) for the neurotransmitter as illustrated in Fig. 2.2 because the experimental analysis still is practically difficult for the molecular process in the cleft. Some mathematical models for the dynamic behavior of ACh in generation of the MEPC at the neuromuscular junction have been proposed to analyze the transient process of the synaptic chemical transmission.

The models may be classified into two groups with respect to the methods employed; one is the differential equation method so that the models are represented with simultaneous differential equations to characterize the dynamic behavior of ACh and the other reactants in the RD system with the respective functions of the concentrations of space and time, and the other approach is the "Monte Carlo method" which characterizes the behavior by specifying the position of each of a number of ACh molecules at a given time (and the state of the receptor molecule if ACh molecule is bound to it). The practical limitations of computational costs are quite different in the two methods, and dependent on the complexity of the problem to be solved; the differential equation method is preferable if the geometry and chemical kinetic scheme used are simple and if high numerical accuracy and analytical generalization are required, while the Monte Carlo method is more practical if one requires realistic modeling

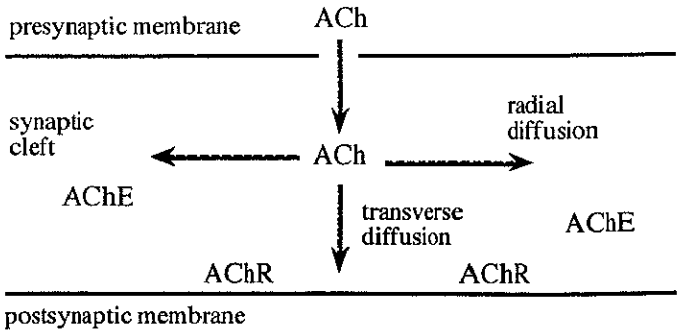


**Fig.2.2.** Reaction-diffusion system for the chemical transmission process in the synaptic cleft.

of specific geometry and chemical kinetics [2]. The models by the differential equation method are further classified with respect to the dimension of the space in which ACh diffuses. On the other hand, the dimension of the space in the Monte Carlo method is usually three because of little effect of the dimension on the computational cost.

The models by the Monte Carlo method are developed by Bartol *et al.* [2] to analyze the effects of three-dimensional structure of the neuromuscular junction on the generation of MEPC. The analysis is performed with regard to the effect of the spacing of the junctional folds and the release of multiple quantal packets of ACh, concluding that increasing the spacing between folds raises the peak current and decreasing the spacing of adjacent quantal release sites increases the potentiation of peak current. The models are also applied to predict the AChE density and the turnover number at frog neuromuscular junction [1] and to analyze the ACh release mechanism called the expanding pore mechanism [29].

The model constructed in this study is the one by the differential equation method with two dimensions in the space, that is, the transverse and radial directions, and the earlier models in the same group provide the basic frames for extension to this two-dimensional compartment model. In the rest of this section representation of RD system for ACh in these earlier models is reviewed.

### 2. The model of Rosenberry

Two kinetic models for the RD system of ACh are introduced by Rosenberry [26] to predict the amplitudes and time courses of EPC and MEPC at the neuromuscular junctions. In the simpler model with homogeneous reaction space by "zero-dimensional" differential equation method, it is assumed that all the reactants (ACh, AChR and AChE) are distributed homogeneously throughout the synaptic reaction space at all times. The diffusion process of ACh in the cleft is approximated with the simple efflux of ACh due to the concentration gradient.

In the models the following scheme is assumed for the interaction of ACh with functionally dimeric AChR:

$$\mathrm{ACh} + \mathrm{R} \underset{k_{-r}}{\overset{2k_r}{\rightleftharpoons}} \mathrm{R_1} \qquad \mathrm{ACh} + \mathrm{R_1} \underset{2k_{-r}}{\overset{k_r}{\rightleftharpoons}} \mathrm{R_2} \tag{2.4}$$

where R and $\mathrm{R_1}$ indicate the AChR species free and singly bound with ACh, respectively,

and the AChR species doubly bound with ACh is denoted by $R_2$. $R_1$ corresponds to closed channel form of AChR, and $R_2$ to an open assembly. Each receptor site in dimeric AChR binds with ACh equivalently and independently by the rate constants of $k_r$ and $k_{-r}$. The reaction of AChE follows the mechanism of Eqn. 2.3. The ACh release into the cleft is assumed to be instantaneous.

Application of the mass-action law to the scheme of AChR and the steady-state approximation to the scheme of AChE leads to a set of rate equations for AChR species. With the further assumption that the concentration of AChR and AChE are in excess of the total ACh released, Rosenberry derives the analytic form of the solution for the time course of $R_2$ concentration, which is supposed to be linearly correlated to generation of EPC or MEPC, as given in:

$$\frac{R_2(t)}{R_T} = \left( \frac{k_r A_0 (e^{-t/\tau_\beta} - e^{-t/\tau_\alpha})}{\tau_\alpha^{-1} - \tau_\beta^{-1}} \right)^2 \tag{2.5}$$

where $A_0$ and $R_T$ denote the initial concentration of ACh and total concentration of AChR species, respectively. $\tau_\alpha$ and $\tau_\beta$ are constants derived from rate constants $k_i$'s ($i = r, -r, 1, -1, 2, 3$), diffusion coefficient of ACh in the cleft, and other constants such as $A_0$, $R_T$, and $E_T$ (total concentration of AChE species). Equation 2.5 accurately predicts the decay constants, but its prediction of the amplitudes and growth times is inaccurate.

Rosenberry improves the homogeneous reaction model to a two-reaction-space model in which the ACh reactions are postulated to occur in two compartments: the first compartment initially contains all the released ACh, while the second compartment receives ACh by diffusion from the first. According to the classification mentioned in the preceding section, the improved model becomes a differential equation model with one dimension in the radial direction.

An analog computer is used to yield the time course of $R_2(t)$ instead of the analytic formula because of the intrinsic nonlinearity contained in the rate equations representing the RD system of the two-compartment model. The model could predict amplitudes and time constants of the EPC within a factor of two in agreement with those observed experimentally. The simulation analysis of the model showed that the amplitudes and time course are primarily determined by the chemical reaction rate of ACh associated with AChR and

AChE and that these interactions occur under nonequilibrium conditions.

The dynamic behavior of ACh in generation of the EPC (or the MEPC) may be appropriately formulated with a diffusion equation with nonlinear reaction terms, accompanied by the rate equations for AChE and AChR as described in the following chapter. The two-compartment model is regarded as a model of the reaction-diffusion equations discretized to just two compartments. Though the time courses generated by these models are still inaccurate because of truncated errors due to numerical analysis method, the ideas introduced with these models are important as the basis of the models followed.

### 3. The model of Wathey

Wathey *et al.* [32] proposed the model classified into the category by the differential equation method with one dimension in space parallel to the pre- and post-synaptic membranes to examine the known quantitative features of nicotinic transmission. In the model the synaptic cleft is represented as the space within the disc of radius $L$ bounded at the top by the presynaptic membrane and at the bottom by the postsynaptic membrane. The radial coordinate $r$ corresponds to the distance from the axis of the disc at which ACh is released instantaneously. It is assumed that AChR and AChE are distributed homogeneously in the disc, and ACh diffuses radially from the center of the disc to the edge of the disc at which ACh flows out due to the concentration gradient. The model is considered as the extension of the two-compartment model by Rosenberry to have enough number of compartments in the radial direction to achieve the accurate analysis.

The same scheme as in the model of Rosenberry is assumed for the interaction of ACh with AChR, while the scheme for the hydrolysis of ACh by AChE is simplified as follows:

$$\mathrm{ACh} + \mathrm{E} \overset{k_1}{\rightarrow} \mathrm{X} \overset{k_3}{\rightarrow} \mathrm{E} + \mathrm{Ch} + \mathrm{acetate} \tag{2.6}$$

where the first reaction is not reversible and X represents several intermediate states.

Application of the mass-action law to the schemes of AChR and of AChE leads to a one-dimensional diffusion equation and rate equations for AChR species as given in:

$$\frac{\partial A}{\partial t} = D\left(\frac{\partial^2 A}{\partial r^2} + \frac{1}{r}\frac{\partial A}{\partial r}\right) - k_1 AE - 2k_r AR + (k_{-r} - k_r A)R_1 + 2k_{-r}R_2$$

$$\frac{dR}{dt} = -2k_r AR + k_{-r}R_1 \tag{2.7}$$
$$\frac{dR_1}{dt} = 2k_r AR - (k_{-r} + k_r A)R_1 + 2k_{-r}R_2$$
$$\frac{dR_2}{dt} = k_r AR_1 - 2k_{-r}R_2$$

where the italic capital letter denotes the concentration of the respective chemical species at point $r$ and time $t$ and $A$ expresses the ACh concentration. $D$ indicates the diffusion coefficient of ACh in the cleft. The total number of $R_2$ at time $t$ is obtained by

$$C(t) = 2\pi \int_0^L R_2(r,t) r dr \tag{2.8}$$

which is assumed to be linearly correlated to generation of the MEPC.

A numerical integration method (finite difference method) is employed to calculate the dynamic behavior of RD system for generation of the MEPC. The simulation with the known parameters reproduces the experimentally measured amplitude, growth time, and the decay constant. The model also simulates voltage and temperature dependencies and effects of inactivating AChE and AChR, demonstrating that the neurotransmitter is buffered by binding to AChR and the postsynaptic response can be potentiated in the absence of AChE.

This model provides a good description of the quantal event at the neuromuscular junction and reassurance of collection of a reasonably complete and self-consistent set of data. Though there remain some limitations such as analysis of the junctional fold and ACh release mechanism because of the assumptions of homogeneous distribution of reactants in the transverse direction and of the instantaneous release of ACh, the model is so useful practically that the similar model is used by Land *et al.* to study the rising phase of an MEPC to derive diffusion coefficient and forward rate constants controlling ACh in the intact neuromuscular junction [15], and is applied to the similar analysis with the empirical data of the falling phase of an MEPC [14]. The model is also employed to analyze the ACh release mechanism, especially to ensure the new data for the growth time of MEPC of 250 $\mu$s [30].

### 4. The model of Friboulet

Friboulet *et al.* [7] constructed the model classified into the category by the differential equation method with one dimension in space along the transverse direction from the presy-

naptic membrane to the postsynaptic membrane. Though it is assumed that the reaction and diffusion occur in the disc representing a space of the cleft as same as for the model of Wathey, the radial diffusion process of ACh is simplified as the homogeneous distribution and the simple efflux at the edge of the disc, while the transverse diffusion process is formulated with diffusion equation. The transverse coordinate $x$ denotes the distance from the presynaptic membrane. The model takes into account the anisotropic distribution of the individual components participating in generation of the MEPC, that is, the homogeneous distribution of AChE and localized distribution of AChR on the postsynaptic membrane. ACh release into the cleft is assumed to be instantaneous.

The schemes expressed by Eqns. 2.2 and 2.3 are assumed for the interaction of ACh with AChR and the hydrolysis of ACh with AChE, respectively. Application of the mass-action law to these schemes leads to a one-dimensional diffusion equation and rate equations for AChR and AChE species as given in:

$$
\begin{aligned}
\frac{\partial A}{\partial t} &= D\frac{\partial^2 A}{\partial x^2} - k_1 AE + k_{-1}X_1 - 2k_r AR + (k_{-r} - k_r A)R_1 + 2k_{-r}R_2 \\
\frac{dE}{dt} &= -k_1 AE + k_{-1}X_1 + k_3 X_2 \\
\frac{dX_1}{dt} &= k_1 AE - (k_{-1} + k_2)X_1 \\
\frac{dX_2}{dt} &= k_2 X_1 - k_3 X_2 \\
\frac{dR}{dt} &= -2k_r AR + k_{-r}R_1 \\
\frac{dR_1}{dt} &= 2k_r AR - (k_{-r} + k_r A)R_1 + 2k_{-r}R_2 \\
\frac{dR_2}{dt} &= k_r AR_1 - (2k_{-r} + k_o)R_2 + k_c R_o \\
\frac{dR_o}{dt} &= k_o R_2 - k_c R_o
\end{aligned}
\tag{2.9}
$$

where $D$ indicates the transverse diffusion coefficient. Under the assumption of the homogeneous distribution of components in a compartment, the total number of the open channel form of AChR and hence the generation of MEPC are linearly correlated to $R_o$.

A numerical integration method (finite difference method) is employed to solve the differential equations. The model predicts the amplitude and time constants in agreement with those observed experimentally, in all the conditions of inhibition of the enzyme or the recep-

tor tested. The model is also applied to examine the influence of the width of the cleft in order to understand what happens when ACh diffuses in junctional folds. When the width is increased by two- and four-fold, the amplitude decreases by about two- and eight-fold, respectively. The response to ACh thus is rapidly reduced when the width increases.

Though this model represents all the interactions of ACh related to the generation of MEPC, it does not include the radial diffusion process in the diffusion equation which has significant effects on generation of the MEPC as demonstrated in Section 4.1. It should be noted that the inclusion of the transverse diffusion process in the model makes it possible to analyze the effect of the junctional fold.

# Chapter 3

# Construction of Compartment Model

As mentioned in Chapter 2, the chemical transmission process of ACh is comprised of the three basic processes: release from the presynaptic membrane accompanied with fusion of the synaptic vesicle, diffusion in the cleft and hydrolysis by AChE, and interaction with AChR for the MEPC generation at the postsynaptic membrane. In this chapter a compartment model for the RD system of ACh in a two-dimensional space of axis-symmetrical disc is constructed for analysis of the diffusion and reaction processes of ACh in the synaptic cleft at the neuromuscular junction. The action of the ACh release mechanisms is formulated as an additional differential equation to express the kinetics of the expanding pore mechanism and the active release mechanism. In the model the junctional fold is simplified as a concentric cylinder with its top surface attached to the bottom of the disc to open a hole to the synaptic cleft at the postsynaptic membrane.

In the RD system ACh concentration varies with time and position in the space of the synaptic cleft, due to transverse and radial diffusion of ACh and its interaction with the AChR and AChE. The behavior of the RD system is expressed by a two-dimensional diffusion equation with nonlinear reaction terms due to the rate processes for AChR and AChE. For simulation under the specified boundary and initial conditions, the method of lines is applied to discretize the partial differential equation with respect to the space variables on the transverse and radial coordinates, resulting in a compartment model represented by a set of nonlinear ordinary differential equations. Based on an optimal selection of the subdivision numbers and critical radius for the simulation, the model for the synapse without the junctional fold minimally comprises a single compartment in the transverse direction and

ten compartments in the radial direction in a disc with 500nm of radius and 50nm of height which specifies a space of the synaptic cleft for generation of the MEPC. In the model for the synapse with the junctional fold the transverse diffusion of ACh needs to be taken into consideration instead of homogeneous concentration in one compartment.

The ordinary differential equations governing the RD system of ACh are numerically integrated with respect to time by the Gear method to yield the spatial and temporal changes in concentrations of ACh in the disc and of the open channel form of AChR at the bottom of the disc. Total number of the open channel form of AChR is assumed to be linearly correlated to generation of the MEPC. Hence, the general idea in the method of lines and the Gear method is also explained in this chapter.

## 3.1 Two-dimensional compartment model

### 1. Formulation of the reaction-diffusion system for ACh

The RD system for ACh as illustrated in Fig. 3.1 is defined for modeling and analysis of the chemical transmission process at the neuromuscular junction for generation of the MEPC. A synaptic vesicle is fused with the presynaptic membrane as a sphere, so that ACh is released through a pore on the presynaptic membrane from the synaptic vesicle of the radius of $R_v$ with the center at $r = 0$. The radius and length of the pore are denoted as $\rho$ and $l$, respectively. The junctional fold is simplified as a concentric cylinder with its top surface attached to the bottom of the disc to open a hole to the synaptic cleft at the postsynaptic membrane, in order to avoid the additional dimension for the RD system. The ACh concentration is assumed to vary with time $t$ and point $(x, r)$ in a two-dimensional space of axis-symmetrical disc of the synaptic cleft (the range of space variables: $0 \leq x \leq w$,

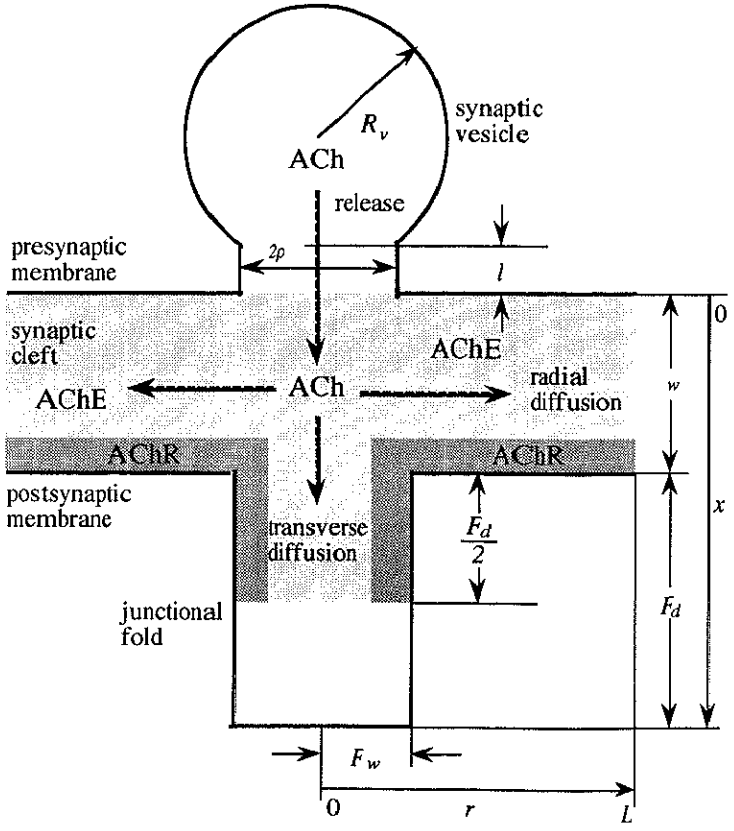


**Fig.3.1.** Reaction-diffusion system for ACh in a two-dimensional space of axis-symmetrical disc of the synaptic cleft. A quantum of ACh molecules is released on the release area with the radius of $d$ from the synaptic vesicle.

$0 \leq r \leq L$) and the concentric cylinder of the junctional fold (the range of space variables: $w \leq x \leq w + F_d$, $0 \leq r \leq F_w$). The radius $L$ of the disc is defined as the extent of a quantal packet of ACh to generate the MEPC, and referred to critical radius [7]. The concentration function $A(x, r, t)$ now represents the behavior of ACh due to influx of ACh through a circular area on the presynaptic membrane ($r \leq d$ [$< L$] on the top surface boundary at $x = 0$), transverse and radial diffusion in the synaptic cleft and the junctional fold, and interactions with AChE (in the light grayed area) and AChR (in the dark grayed area).

The RD system for ACh in the synaptic cleft is thus expressed by a two-dimensional diffusion equation with nonlinear reaction terms, accompanied by the rate equations for AChE and AChR as follows:

$$
\begin{aligned}
\frac{\partial A}{\partial t} &= D_t \frac{\partial^2 A}{\partial x^2} + D_r \left( \frac{\partial^2 A}{\partial r^2} + \frac{1}{r} \frac{\partial A}{\partial r} \right) + \delta(x) u(d - r) \frac{dS}{dt} \\
&\quad - k_1 AE + k_{-1} X_1 - 2k_r AR + (k_{-r} - k_r A) R_1 + 2k_{-r} R_2 \\
\frac{dE}{dt} &= -k_1 AE + k_{-1} X_1 + k_3 X_2 \\
\frac{dX_1}{dt} &= k_1 AE - (k_{-1} + k_2) X_1 \\
\frac{dX_2}{dt} &= k_2 X_1 - k_3 X_2 \\
\frac{dR}{dt} &= -2k_r AR + k_{-r} R_1 \\
\frac{dR_1}{dt} &= 2k_r AR - (k_{-r} + k_r A) R_1 + 2k_{-r} R_2 \\
\frac{dR_2}{dt} &= k_r AR_1 - (2k_{-r} + k_o) R_2 + k_c R_o \\
\frac{dR_o}{dt} &= k_o R_2 - k_c R_o
\end{aligned}
\tag{3.1}
$$

where $D_t$ and $D_r$ indicate the diffusion coefficients for ACh in the transverse and radial directions, respectively. It is supposed that the release of ACh from a synaptic vesicle takes place in the circular area with the radius of $d$. $\delta(x)$ and $u(r)$ represent a delta function and a step function, respectively. The reaction terms are derived from Eqns. 2.2 and 2.3 by application of the mass-action law. The behavior of Ch and acetate is not considered in the formulation because this analysis is mainly concerned with the dynamic behavior of ACh in the RD system which is most relevant to evolution of the MEPC.

The ACh release mechanisms of the expanding pore and the acceleration are formulated

in a following differential equation to represent the change of ACh concentration in the synaptic vesicle, that is, the influx rate of ACh to the circular area:

$$\frac{dS(t)}{dt} = \frac{aD_p\pi\rho(t)^2}{Vl}(S(t) - \overline{A(0,r,t)}) \qquad \rho(t) = min(b_0 + bt, R_v) \tag{3.2}$$

where $\overline{A(0,r,t)}$ and $S(t)$ express the mean concentrations of ACh at time $t$ over the release area ($A(0,r,t)$ for $r \leq d$) and in the synaptic vesicle, respectively. $D_p$ is the diffusion coefficient of ACh in the pore. $V$ is the constant volume of the vesicle of $4/3\pi R_v^3$ and $l$ is the length of the pore. $\rho(t)$ denotes the radius of the pore at time $t$ which extends at a rate $b$ from $b_0$ to $R_v$, the radius of the synaptic vesicle. The parameter $a$ designates the acceleration rate for the active release mechanism.

The boundary conditions for ACh are expressed by

$$\begin{aligned}
\frac{\partial A(x,r,t)}{\partial x} &= 0 \quad \text{at } x = 0,\ x = w \text{ for } r \geq F_w,\ x = w + F_d \text{ for } r \leq F_w \\
\frac{\partial A(x,r,t)}{\partial r} &= 0 \quad \text{at } r = 0,\ r = F_w \text{ for } w \leq x \leq w + F_d \\
A(x,r,t) &= 0 \quad \text{at } r = L \text{ for } x \leq w
\end{aligned} \tag{3.3}$$

so that ACh cannot leak out at the boundaries of the disc and the cylinder other than the side surface of the disc where ACh is removed by radial diffusion. There initially exist no ACh inside the disc. The total number of the open channel form of AChR is obtained by

$$C(t) = 2\pi \int_{F_w}^{L} R_o(w,r,t) r dr + 2\pi F_w \int_{w}^{w+F_d} R_o(x,F_w,t) dx \tag{3.4}$$

which is assumed to be linearly correlated to generation of the MEPC.

## 2. Discretization of the reaction-diffusion system

The partial differential equation governing the RD system for ACh in Eqn. 3.1 is numerically solved under the specified boundary and initial conditions to reveal the behavior of the system after the release of ACh into the synaptic cleft. For this simulation the method of lines [27] is applied to discretize the partial differential equation with respect to the space variables for the transverse and radial coordinates. The set of rate equations thus derived for ACh, AChE and AChR comprises a compartment model, which is numerically integrated with respect to time by the Gear method [8, 16] to yield for the analysis the spatial and temporal changes

in concentrations of ACh in the disc and in the cylinder, and of the open channel form of AChR at the bottom of the disc and at the side surface of the cylinder. The procedure of the discretization is described below in a rather simple case of $F_w = 0$ (foldless) and $a = \infty$ (instantaneous release of ACh). The representations of the other cases of the compartment models are described in the form of MatLab's S-functions [16] in Appendix.

The system of differential equations representing the RD system for ACh (Eqn. 3.1) may be expressed in a simplified form:

$$\begin{aligned} A_t &= \alpha A_{xx} + \beta(A_{rr} + \frac{1}{r}A_r) + f(A, Y_1, \ldots, Y_n) \\ (Y_k)_t &= g_k(A, Y_1, \ldots, Y_n) \qquad\qquad k = 1, 2, \ldots, n \end{aligned} \tag{3.5}$$

with the boundary conditions

$$\begin{aligned} A_x &= 0 \quad \text{at} \quad x = 0 \quad \text{and} \quad x = w\,; \\ A_r &= 0 \quad \text{at} \quad r = 0 \quad \text{and} \quad A = 0 \quad \text{at} \quad r = L \end{aligned}$$

The function $A(x, r, t)$ is discretized to $N_t \times N_r$ functions $\{A_{i,j}(t);\ i = 1, 2, \ldots, N_t,\ j = 1, 2, \ldots, N_r\}$ with $N_t - 1$ points spaced by $\delta x = w/N_t$ on the transverse coordinate and $N_r - 1$ points spaced by $\delta r = L/N_r$ on the radial coordinate. Replacement of the space derivatives with the following standard finite-difference approximations,

$$\begin{aligned} A_{xx} &= \frac{A_{i-1,j} - 2A_{i,j} + A_{i+1,j}}{(\delta x)^2} \\ A_{rr} &= \frac{A_{i,j-1} - 2A_{i,j} + A_{i,j+1}}{(\delta r)^2} \\ A_r &= \frac{A_{i,j+1} - A_{i,j-1}}{2\delta r} \end{aligned} \tag{3.6}$$

leads to the system of ordinary differential equations as follows:

$$\begin{aligned} (A_{i,j})_t &= \frac{\alpha}{(\delta x)^2}(A_{i-1,j} - 2A_{i,j} + A_{i+1,j}) \\ &\quad + \frac{\alpha}{(\delta r)^2}\{A_{i,j-1} - 2A_{i,j} + A_{i,j+1} + \frac{A_{i,j+1} - A_{i,j-1}}{2(j + 0.5)}\} \\ &\quad + f(A_{i,j}, (Y_1)_{i,j}, \ldots, (Y_n)_{i,j}) \\ (Y_{ki,j})_t &= g_k(A_{i,j}, (Y_1)_{i,j}, \ldots, (Y_n)_{i,j}) \end{aligned} \tag{3.7}$$

for $i = 1, 2, \ldots, N_t$, $j = 1, 2, \ldots, N_r$ and $k = 1, 2, \ldots, n$. The boundary conditions are treated as the values of $A$ at the additional points:

$$A_{0,j}(t) = A_{1,j}(t) \quad \text{and} \quad A_{N_t+1,j}(t) = A_{l,j}(t) \quad \text{for} \quad \text{all } j \text{ and } t > 0$$
$$A_{i,0}(t) = A_{i,1}(t) \quad \text{and} \quad A_{i,N_r+1}(t) = 0 \quad \text{for} \quad \text{all } i \text{ and } t > 0$$

### 3. Values of parameters

The following values of the kinetic parameters are used for the simulation throughout this study:

$$k_r = 30\text{mM}^{-1}\text{msec}^{-1}, k_{-r} = 10\text{msec}^{-1}, k_o = 20\text{msec}^{-1}, k_c = 5.0\text{msec}^{-1};$$
$$k_1 = 200\text{mM}^{-1}\text{msec}^{-1}, k_{-1} = 1.0\text{msec}^{-1}, k_2 = 110\text{msec}^{-1}, k_3 = 20\text{msec}^{-1}$$

and the other parameters are summarized in Table 3.1 [7]. The following values of the structural parameters [12] are also used:

$$b_0 = 1.0\text{nm}, R_v = 18.5\text{nm}, l = 10.0\text{nm}$$

Though it is natural that the radius of the ACh release area ($d$) is set to be the same value of the radius ($\rho(t)$) of the pore formed on the presynaptic membrane, the value of 50nm is assigned for $d$ because of the difficulty in the representation of its time dependency in the compartment model. The value of 50nm for $d$ is equal to the value of the width of the cleft ($w$), and this assignment is based on the consideration that the ACh molecules released through the pore of tiny radius spread over the cylindrical space in the cleft when

**Table 3.1** Values of parameters for construction of the model

| parameter | notation | value used |
|---|---|---|
| Volume of the synaptic cleft | $V_c$ | $450\mu\text{m}^3$ |
| Width of the synaptic cleft | $w$ | 50nm |
| Total ACh released per MEPC | $N_A$ | $10^4$molecules |
| Total AChE in the synaptic cleft | $N_E$ | $2\times10^7$sites |
| Surface density of AChR | $C_R$ | $2\times10^4\mu\text{m}^{-2}$ |

they reach the postsynaptic membrane by the diffusion process. The radius of the cylindrical space could be estimated equal to the distance in which the ACh molecules diffuse in the transverse direction. The value for the critical radius ($L$) is evaluated in the following section in association with the effects of the diffusion coefficient of ACh.

The value for $E_T$ (total concentration of AChE at a point; $= E + X_1 + X_2$) is set to $74\mu$M, which is derived by

$$E_T = \frac{N_E}{V_c N} \tag{3.8}$$

where $N$ indicates Avogadro's number. The value for $R_T$ (total concentration of AChR at a point; $= R + R_1 + R_2 + R_o$) in the disc is obtained from the surface density of the AChR ($C_R$), the width of the synaptic cleft ($w$), and the subdivision numbers on the transverse coordinate ($N_t$) so that

$$R_T = \frac{C_R \times (\text{Area of the disc})}{(\text{Area of the disc}) \times (w/N_t) \times N} = \frac{C_R N_t}{wN} \tag{3.9}$$

The value for $R_T$ in the cylinder representing the junctional fold is dependent on the critical radius ($L$), the subdivision number on the radial coordinate ($N_r$), and the radius of the cylinder as follows:

$$\begin{aligned} R_T &= \frac{C_R \times (\text{Area of the side surface of cylinder with AChR})}{(\text{Volume of space with AChR in cylinder}) \times N} \\ &= \frac{C_R N_r' N_r}{(N_r' - 0.5) LN} \end{aligned} \tag{3.10}$$

where $N_r'(= N_r \times F_w/L)$ is the subdivision number on the radial coordinate in the cylinder. For example, the value of $R_T$ is 2.0mM for the compartment model with the parameters of $L = 500$ nm, $N_r = 10$, $N_t = 3$, $F_w = 0$ (foldless) and $a = \infty$ (instantaneous release of ACh) which is employed for the analysis of the diffusion process of ACh in the synaptic cleft.

The initial concentration of ACh in the synaptic vesicle ($S(0)$) is obtained by

$$S(0) = \frac{N_A}{VN} \tag{3.11}$$

where $V$ $(= 4/3\pi R_v^3)$ denotes the volume of a synaptic vesicle. For the special case of $a = \infty$ (instantaneous release of ACh) assumed, $S(0)$ is replaced with the initial concentration of ACh for the release area ($A(0, r, 0)$ for $r \leq d$) as given by

$$A(0, r, 0) = \frac{N_A N_t}{\pi d^2 wN} \tag{3.12}$$

which results in 127mM for the compartment model mentioned above as the example.

The accurate value of the diffusion coefficient of ACh in the milieu of the synaptic cleft is unknown, so that the analysis is performed in the range between $0.25 \sim 4.0$ ($\times 10^{-6}\mathrm{cm}^2\mathrm{sec}^{-1}$) for $D_t$ and $D_r$, which contains all the presumable values described in Section 2.2.

### 4. Appropriate radius of the disc and number of compartments

In construction of a two-dimensional compartment model for the RD system formulated above, the radius $L$ of the disc and the subdivision numbers of $N_t$ on the transverse coordinate and $N_r$ on the radial coordinate are the parameters to be chosen for optimal representation of the behavior of the model. The subdivision numbers are relevant to the validity for reduction of the space dimension in the previous models described in Section 2.3. A single copartment on the transverse coordinate ($N_t = 1$) means the homogenous distribution of reactants in the transverse direction as assumed in the models of Rosenberry [26] and of Wathey [32], while a single compartment on the radial coordinate ($N_r = 1$) indicates the homogeneity in the radial direction as the case in the model of Friboulet [7]. Furthermore, the assumption of the instantaneous release of ACh into the cleft corresponds to the case that the parameter $a$ in the release mechanism described in the preceding section is set to be infinite. For example, the one-dimensional compartment model of Friboulet arises as the case of $L = 300\mathrm{nm}$ ($= d$), $F_w = 0$ (foldless), $N_t = 10$, $N_r = 1$, $D_t = 2.0 \times 10^{-6}\mathrm{cm}^2\mathrm{sec}^{-1}$, $D_r = 5.9 \times 10^{-7}\mathrm{cm}^2\mathrm{sec}^{-1}$ (i.e., the apparent diffusion rate constant as $1.3 \times 10^{-3}\mathrm{sec}^{-1}$), and $a = \infty$.

The optimal selection of $L$, $N_t$ and $N_r$ is evaluated with reference to the relative variation in $C(t;\alpha)$, the total number of $R_o$ (open channel form of AChR), due to parameter change from $\alpha_1$ to $\alpha_2$, i.e., by a quantity,

$$V_r = \frac{\int |C(t;\alpha_2) - C(t;\alpha_1)|\, dt}{\int C(t;\alpha_1) dt} \tag{3.13}$$

where $C(t;\alpha)$ is obtained by Eqn. 3.4 with the parameter value of $\alpha$. The optimal value of the parameter is determined to be $\alpha_1$ when the value of $V_r$ becomes negligible. Details of the error estimation by $V_r$ are discussed in the following section.

The evaluation of the optimal values for the parameters begins with the model without the junctional fold. The radius $L$ of the disc is defined as the extent of a quantal packet of

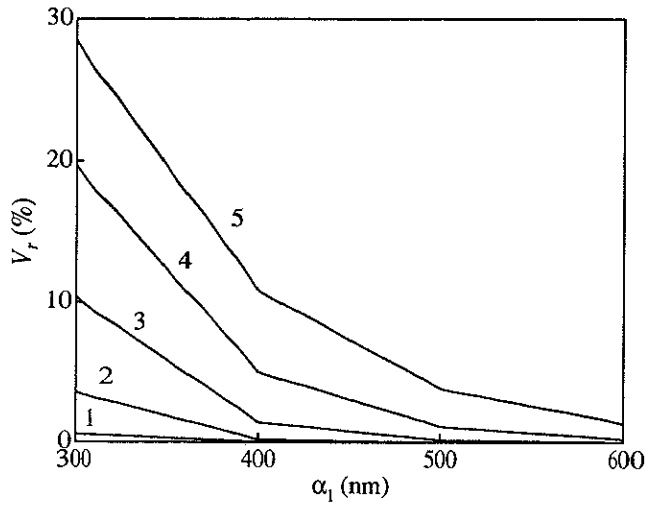


**Fig.3.2.** Effect of the critical radius of the disc on the response of the open channel form of AChR. The variation $V_r$ is evaluated for increase by 100nm in each of the radius $L$ (in nm) of 300, 400, 500 and 600 indicated on the abscissa. The number on a curve corresponds to the value of $D_t\,(=D_r)$ (in $10^{-6}\mathrm{cm}^2\mathrm{sec}^{-1}$): 1: 0.25, 2: 0.5, 3: 1.0, 4: 2.0, and 5: 4.0.

ACh to generate the MEPC, and referred to critical radius [7]. Figure 3.2 shows the behavior of the variation $V_r$ with increase by 100nm in $L$ (i.e., $\alpha_2 = \alpha_1 + 100$) at every 100nm for $\alpha_1$ (as $L$) between 300nm and 600nm. Evaluation of $V_r$ results from the simulation of the

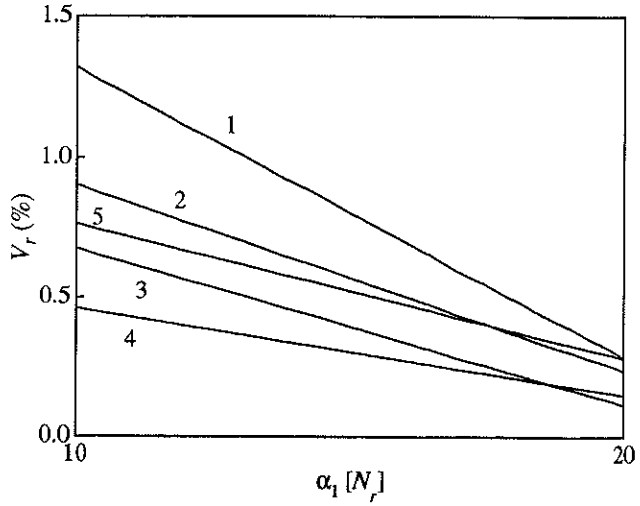


**Fig.3.3.** Effect of the compartment number in the radial direction on the response of the open channel form of AChR. The variation $V_r$ is evaluated for increase in the compartment number $N_r$ from 10 to 20 and from 20 to 30. The number on a curve corresponds to the value of $D_t\,(=D_r)$ (in $10^{-6}\mathrm{cm}^2\mathrm{sec}^{-1}$): 1: 0.25, 2: 0.5, 3: 1.0, 4: 2.0, and 5: 4.0.

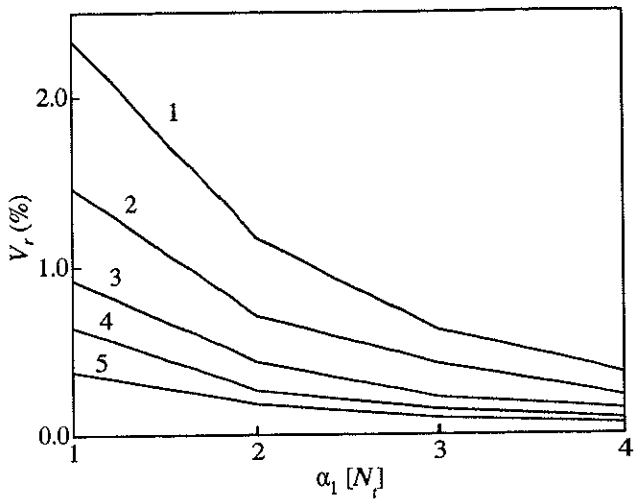


**Fig.3.4.** Effect of the compartment number in the transverse direction on the response of the open channel form of AChR. The variation $V_r$ is evaluated for increase by one in each of the compartment number of $N_t$ of 1, 2, 3, 4 indicated on the abscissa. The number on a curve corresponds to the value of $D_t\,(=D_r)$ (in $10^{-6}\mathrm{cm}^2\mathrm{sec}^{-1}$): 1: 0.25, 2: 0.5, 3: 1.0, 4: 2.0, and 5: 4.0.

RD system for each value of $L$ (= 300, 400, 500, 600, and 700 in nm) and various diffusion coefficients (i.e., $D_t = D_r = 0.25 \sim 4.0$ ($\times 10^{-6}\mathrm{cm}^2\mathrm{sec}^{-1}$)). For the simulation $N_t$ is set at 3; the three compartments correspond to the phases of release, diffusion, and generation of the MEPC, respectively, while $N_r$ varies from 6 to 14 according to $N_r = L/d$ with the maximum size of compartment fixed equal to $d$ (= 50nm). It follows from the behavior of $V_r$ decreasing to 0 in Fig. 3.2 that increase in $L$ has the temporal variation of $C(t;L)$ converge to a common curve, and that the higher diffusion coefficient requires the larger radius. It is thus concluded that the appropriate value of $L$ for the model is at least 500nm, at which the variation in $L$ causes the temporal change of $C(t;L)$ to deviate merely within 1.2% for most of the diffusion coefficient in the variation range.

The compartment number in the radial direction is now determined by analysis of the effect of subdivision number $N_r$ on $V_r$ with $C(t;N_r)$. It should be noted that the compartment number corresponds to the minimal element number resulting from discretization of the spatial coordinate in the method of lines [27] to assure an acceptable accuracy for the simulation (numerical integration of the partial differential equation). For $L$ = 500nm and $d$ = 50nm chosen, discretization of the radial coordinate in ten elements is at least required

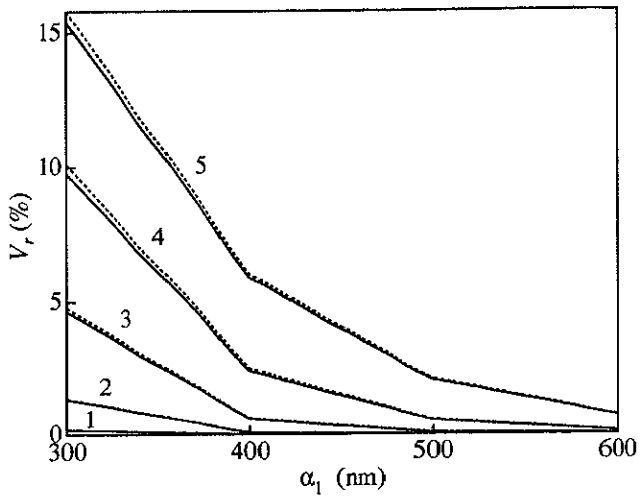


**Fig.3.5.** Effect of the critical radius of the disc on the response of the open channel form of AChR in the cleft with the junctional fold. Solid lines: $V_r$ for the junctional fold with $F_w = 50$nm and $F_d = 500$nm; broken lines: $V_r$ for the junctional fold with $F_w = 50$nm and $F_d = 1000$nm. The variation $V_r$ is evaluated for increase by 100nm in each of the radius $L$ (in nm) of 300, 400, 500 and 600 indicated on the abscissa. The number on a curve corresponds to the value of $D_t (= D_r)$ (in $10^{-6}$cm$^2$sec$^{-1}$): 1: 0.25, 2: 0.5, 3: 1.0, 4: 2.0, and 5: 4.0.

to analyze the behavior in the radial diffusion process. The effect of increase in $N_r$ from 10 ($\alpha_1$) to 20 ($\alpha_2$) and 20 ($\alpha_1$) to 30 ($\alpha_2$) on $V_r$ is demonstrated in Fig. 3.3, where the variation is noticeable for $N_r = 10$, but seems to have no simple dependence on the value of diffusion coefficient. The value of $N_r$ should thus be taken as at least 10 for the model and the value of diffusion coefficient may be chosen arbitrarily since $V_r$ is always less than 1.33%.

As seen in Fig. 3.4, the subdivision number $N_t$ has the effect on the variation $V_r$ somewhat similar to that by $L$. Increase of one element at every element ($\alpha_1$) between 1 and 4 on the transverse coordinate leads to convergence of $C(t; N_t)$ to a common curve, but $V_r$ is less than 2% with most of the diffusion coefficient in the variation range. For simpler modeling, therefore, even the homogeneous state is apparently possible in the transverse direction.

It is hence concluded that the appropriate values of the parameters are $L \geq 500$nm, $N_t \geq 1$ and $N_r \geq 10$ with which the model sufficiently represents the dynamic behavior of the RD system for the chemical transmission process in the two-dimensional space of the synaptic cleft in the case without the junctional fold.

It is also assured that the compartment model with $L \geq 500$nm, $N_t \geq 3$ and $N_r \geq 10$

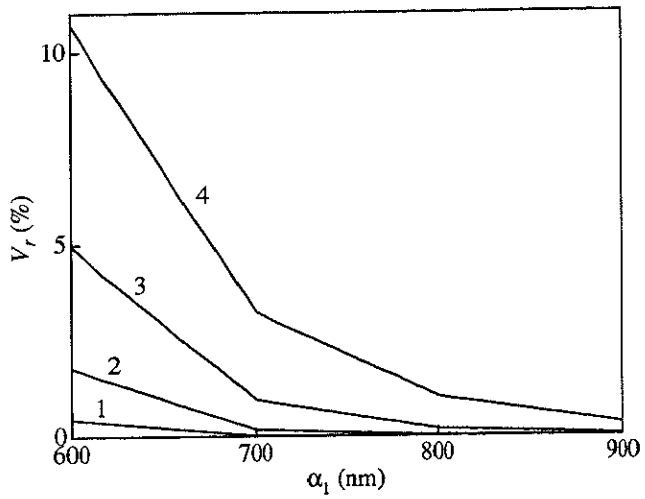


**Fig.3.6.** Effect of the critical radius of the disc with the large ACh release area ($d = 500nm$) on the response of the open channel form of AChR. The variation $V_r$ is evaluated for increase by 100nm in each of the radius $L$ (in nm) of 600, 700, 800 and 900 indicated on the abscissa. The number on a curve corresponds to the value of $D_t\,(= D_r)$ (in $10^{-6}\mathrm{cm}^2\mathrm{sec}^{-1}$): 1: 0.5, 2: 1.0, 3: 2.0, and 4: 4.0.

represents properly the RD system of the synaptic cleft with junctional fold. It should be noted that the cylinder representing the junctional fold is divided into the compartments by the same size in the disc, that is, $N_t \times F_d/w$ and $N_r \times F_w/L$ on the transverse and the radial coordinates, respectively. The applicability of the model is evaluated against the various diffusion coefficients and the different junctional folds (cylinders) with the radius ($F_w = 0$ (foldless), 50nm or 100nm) and the depth ($F_d = 500$nm or 1000nm) using the same procedure for the system without the fold. Figure 3.5 demonstrates the behavior of the variation $V_r$ with increase by 100nm in $L$ (i.e., $\alpha_2 = \alpha_1 + 100$) at every 100nm for $\alpha_1$ (as $L$) between 300nm and 600nm. The attachment of the cylinder to the disc reduces the value of $V_r$ to almost half of that in the foldless case (as shown in Fig. 3.2) regardless of the depth of the cylinder. For all the combinations examined on the diffusion coefficients of ACh and the different junctional folds, the values of $V_r$ are lower than 3.5% with the parameters of $L = 500$nm, $N_t = 3$ and $N_r = 10$, concluding that the model is applicable to the RD system for the synaptic cleft with the junctional fold.

Though the radius $d$ of the release area of ACh is 50nm in these compartment models, the variation in $d$ up to 500nm will be required for examination of the effect of the localized

release of ACh in Section 5.2. It is expected that the larger radius of the release area requires the larger critical radius ($L$), so that the optimal value for $L$ is evaluated again with $d = 500$nm. Figure 3.6 displays the behavior of the variation $V_r$ with increase by 100nm in $L$ between 600nm and 900nm. For the simulation $N_t$ is set at 1 (homogeneous distribution of ACh in the transverse direction), while $N_r$ varies from 24 to 40 according to $N_r = L/25$. This number of 25(nm) is the minimum radius of the release area of ACh for the simulation. It follows from the behavior of $V_r$ decreasing to 0 in Fig. 3.6 that increase in $L$ has the temporal variation of $C(t; L)$ converge to a common curve, and that the higher diffusion coefficient requires the larger radius. It is thus concluded that the optimal value of $L$ for the model is 800nm, at which the variation in $L$ causes the temporal change of $C(t; L)$ to deviate merely within 2% for any diffusion coefficient in the variation range.

## 3.2 Simulation method

### 1. General idea of method of lines

The method of lines has widely been accepted as a method for approximate solution of partial differential equations [9, 27]. The general idea of the method is described as follows.

Let the problem to be solved be given by

$$u_t = f(t, x, u, u_x, u_{xx}) \quad \text{for} \quad 0 \leq x \leq 1 \quad \text{and} \quad t > 0 \tag{3.14}$$

with the initial conditions

$$u(x, 0) = u_0(x) \quad \text{for} \quad 0 \leq x \leq 1$$

and boundary conditions

$$\text{either: } u(0, t) = a(t) \quad \text{or : } u_x(0, t) = g_1(t, u) \qquad \text{for} \quad t > 0 \quad \text{at} \quad x = 0$$

and

$$\text{either: } u(1, t) = b(t) \quad \text{or : } u_x(1, t) = g_2(t, u) \qquad \text{for} \quad t > 0 \quad \text{at} \quad x = 1$$

In the method of lines the interval $0 \leq x \leq 1$ is subdivided into $m$ discrete elements $[x_{j-1}, x_j]\,(j = 1, 2, \ldots, m; x_0 = 0, x_m = 1)$ and the solution $u(x, t)$ is approximated by a vector of $m + 1$ functions $\{u_0(t), u_1(t), \cdots, u_m(t)\}^T$ where the $u_j(t)$ are functions of the single variable $t$ to express $u(x_j, t)$. Derivatives with respect to $x$ are approximated by finite difference relationships between neighboring functions of $u_j(t)$, resulting in a simultaneous system of ordinary differential equations.

For example, consider the heat equation,

$$u_t = u_{xx} \quad \text{for } 0 \leq x \leq 1 \quad \text{and } t > 0 \tag{3.15}$$

with

$$\begin{aligned} u(x, 0) &= u_0(x), \qquad 0 \leq x \leq 1, \\ u(0, t) &= u(1, t) = 0, \qquad t > 0 \end{aligned}$$

which is discretized to $m - 1$ functions $\{u_j(t); j = 1, 2, \ldots, m - 1\}$ with respect to $m - 1$ points spaced by $\delta x = 1/m$. The functions $u_0(t)$ and $u_m(t)$ are known to be zero for all $t$

from the boundary conditions. $(u_j)_{xx}$ are replaced by standard second-order finite difference approximations,

$$\begin{aligned} (u_1)_{xx} &= \frac{-2u_1 + u_2}{(\delta x)^2} \\ (u_j)_{xx} &= \frac{u_{j-1} - 2u_j + u_{j+1}}{(\delta x)^2} \qquad j = 2, 3, \cdots, m-2, \\ (u_{m-1})_{xx} &= \frac{-2u_{m-2} + u_{m-1}}{(\delta x)^2} \end{aligned} \tag{3.16}$$

leading to the equations in matrix-vector form

$$u' = \frac{1}{(\delta x)^2} A u, \tag{3.17}$$

where

$$A = \begin{pmatrix} -2 & 1 & & & & & \\ 1 & -2 & 1 & & & 0 & \\ & 1 & -2 & 1 & & & \\ & & \cdot & \cdot & \cdot & & \\ & & & \cdot & \cdot & \cdot & \\ & 0 & & & 1 & -2 & 1 \\ & & & & & 1 & -2 \end{pmatrix}$$

Hence, an approximate solution to Eqn. 3.15 can be obtained by solving the initial value problem in ordinary differential equations given by Eqn. 3.17 and the initial conditions

$$u(0) = \{u_0(x_1), u_0(x_2), \ldots, u_0(x_{m-1})\}^T,$$

where $x_j = j/m$ for $j = 1, 2, \ldots, m-1$.

Considerable attention has been devoted to solution of initial value problems in ordinary differential equations and many methods are available, including techniques for step size modification to keep local discretization errors within a given tolerance and to ensure the stability of the solution. It is difficult, however, to deal with these adaptive stepsize and stability in the standard finite difference approach to partial differential equations.

Moreover, it should be mentioned that the derived system of ordinary differential equations could be stiff. The stiffness of the system depends on the size of spacing between "the lines", or functions $u_j(t)$, that is, $\delta x$ in Eqn. 3.17. A small local truncation error in the space discretization requires a small $\delta x$, resulting in the large negative eigenvalues of matrix

$A/(\delta x)^2$ as obtained by

$$\lambda_j = \frac{-4\sin^2\{j\pi/(2m)\}}{(\delta x)^2} \qquad j = 1, 2, \cdots, m-1 \tag{3.18}$$

with a stiffness ratio $r$ given by

$$r = \frac{\sin^2\{(m-1)\pi/(2m)\}}{\sin^2\{\pi/(2m)\}} \tag{3.19}$$

or

$$r \approx \frac{4m^2}{\pi^2}$$

for large value of $m$. Choosing $m = 10$, corresponding to a space discretization of 0.1, leads to the stiffness ratio of approximately 40, while, more practically, choosing $m = 100$ yields approximately $r = 4050$. This value is certainly large enough to require a method specially developed for the stiff problems.

## 2. Gear method

The functions $f$ and $g_k$ in Eqn. 3.5 representing the reaction terms of ACh with AChE and AChR give rise to the stiff problem, which is a common feature in kinetic expression of chemical reaction systems to cause great difficulty in the numerical integration. The method of lines itself also requires stiff stable method for the numerical integration of the derived equations as mentioned in the preceding section. Stiff problems have been extensively studied for many years and the most successful algorithms available at present are based on the Gear method [9, 16], which is employed to solve the derived system of ordinary differential equations in this study.

A system of ordinary differential equations is written as

$$\frac{dy(t)}{dt} = f(y, t) \tag{3.20}$$

where $y$ and $f$ are vectors of $\{y^1, y^2, \cdots, y^n\}^T$ and $\{f^1, f^2, \cdots, f^n\}^T$, respectively. The Gear method is a kind of the predictor-corrector methods. The formulas of order $q$ for Eqn. 3.20 are given by

$$\begin{aligned} \text{Predictor} \quad &: \quad y_{n,(0)} = \sum_{i=1}^{q} \alpha_i y_{n-i} + \eta_1 h y'_{n-1} \\ \text{Corrector} \quad &: \quad y_{n,m+1} = \sum_{i=1}^{q} \alpha_i^* y_{n-i} + \eta_0^* h f(y_{n,(m)}, t_n) \end{aligned} \tag{3.21}$$

where the coefficients $\alpha_i$, $\alpha_i^*$, $\eta_1$ and $\eta_0^*$ are evaluated in the text [8]. The values of $[y_{n-1}, hy'_{n-1}, y_{n-2}, \cdots, y_{n-q}]$ are used to determine the predictor $y_{n,(0)}$. As the initial condition specifies only $y_0$ and $hy'_0$, the computation starts with the first-order formula ($q = 1$), then the order increases subsequently up to 5 that is the maximum order assured for the stiff stability.

The convergent solution of the corrector equation is obtained using the Newton method as follows:

$$\begin{aligned} y_{n,(m+1)} &= y_{n,(m)} + \{I - h\eta_0^* J(y_{n,(m)}, t_n)\}^{-1} \\ &\quad \times \left\{ \sum_{i=1}^{q} \alpha_i^* y_{n-i} + h\eta_0^* f(y_{n,(m)}, t_n) - y_{n,(m)} \right\} \end{aligned} \tag{3.22}$$

where the iteration starts with $y_{n,(0)}$ evaluated in the predictor. The Jacobian $J$ of Eqn. 3.20 changes so slow that $J$ would be computed only if the convergence of Eqn. 3.22 should not be attained after three iterations.

The method thus provides the stable numerical solution of a stiff differential equation for relatively large step-size $h$ and the results accumulated so far have proved its applicability to various problems.

### 3. Error estimation by the quantity $V_r$

The method of global error estimation for the method of lines has been proposed especially for parabolic equations in one-dimensional space [3, 4]. Though the method could be applied with its extension to two-dimensional space, rather practical method is used in this study to estimate the global error due to the subdivision numbers of $N_t$ and $N_r$. This method is also applicable to estimate the global error induced by the critical radius of $L$ by mean of the difference between $C(t)$ calculated in the model with the finite critical radius and that with the ideal infinite space.

The quantity $V_r$ introduced in Section 3.1 is a local relative error. Estimation of the global relative error $E(\alpha)$ may be possible by formulation similar to the local relative error $V_r$:

$$E(\alpha) = \frac{\int |C(t;\alpha) - C(t;\infty)|\, dt}{\int C(t;\infty) dt} \tag{3.23}$$

Let $P(\alpha)$ be defined as

$$P(\alpha) = \int C(t;\alpha) dt \tag{3.24}$$

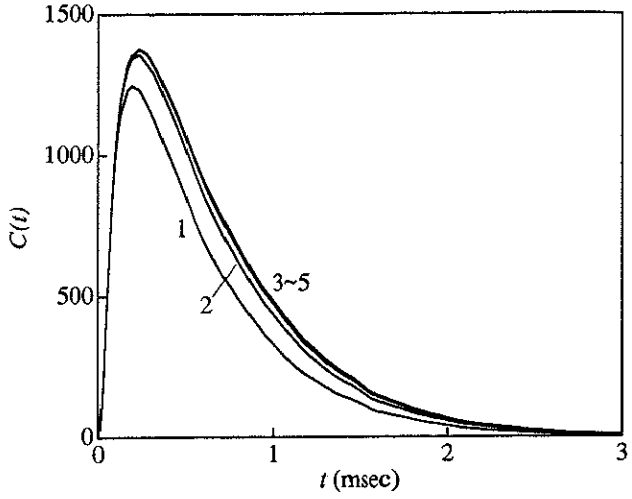


**Fig.3.7.** Monotonic characteristics in the response of the total number of the open channel form of AChR. The number on a curve corresponds to the critical radius of $L$ (in nm) : 1: 300, 2: 400, 3: 500, 4: 600, and 5: 700. The unit of $C(t)$ on the ordinate is the number of the open channel form of AChR. $D_t\,(=D_r) = 2.0 \times 10^{-6}\mathrm{cm}^2\mathrm{sec}^{-1}$.

and suppose that $C(t;\alpha)$ is a monotonically increasing function with respect to $\alpha$ for all $t$ as:

$$\forall t\ (\alpha_1 < \alpha_2 \rightarrow C(t;\alpha_1) < C(t;\alpha_2))$$

Then $P(\alpha)$ too is a monotonically increasing function. This assumption is presumable for $C(t;\alpha)$ yielded in this study. In fact, almost all of the behavior of $C(t;\alpha)$ calculated with respect to variations in $N_t$, $N_r$ or $L$ turn out to be monotonous as demonstrated in Fig. 3.7. The case of the monotonically decreasing function is discussed later.

The local and global errors are expressed with the function $P(\alpha)$ as follows:

$$V_r(\alpha) = \frac{P(\alpha+\Delta)-P(\alpha)}{P(\alpha)} \tag{3.25}$$

$$E(\alpha) = \frac{P_\infty - P(\alpha)}{P_\infty} \tag{3.26}$$

where $\Delta$ and $P_\infty$ denote the increment of $\alpha$ and $P(\infty)$, respectively. The typical $P(\alpha)$ with $C(t)$ calculated in this study allows us to assume

$$E(\alpha+\Delta) = kE(\alpha) \tag{3.27}$$

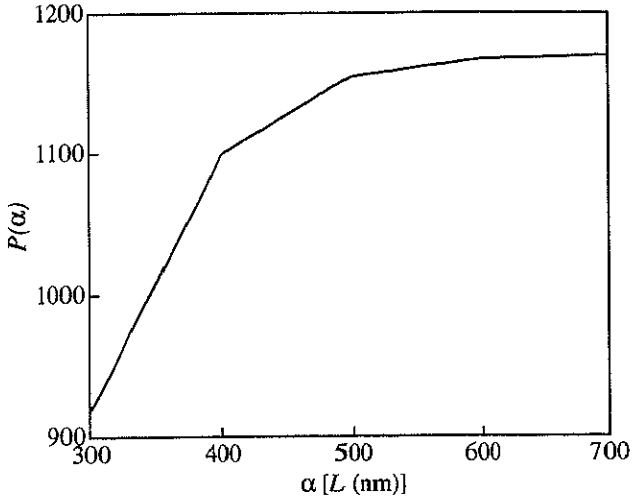


**Fig.3.8.** Relationship of $P(\alpha)$ with the critical radius $L$. $C(t)$ is obtained for the diffusion coefficient $D_t\,(=D_r) = 2.0 \times 10^{-6}\mathrm{cm}^2\mathrm{sec}^{-1}$.

as demonstrated in Fig.3.8. By Eqns. 3.26 and 3.27, Eqn. 3.25 yields

$$V_r(\alpha) = \frac{(1-k)E(\alpha)}{1-E(\alpha)} \tag{3.28}$$

Let $v_1$ and $v_2$ be the values of $V_r$ at $\alpha_1$ and $\alpha_2$ $(=\alpha_1+\Delta)$, respectively:

$$V_r(\alpha_1) = \frac{(1-k)E(\alpha_1)}{1-E(\alpha_1)} = v_1 \tag{3.29}$$

$$V_r(\alpha_2) = \frac{(1-k)kE(\alpha_1)}{1-kE(\alpha_1)} = v_2 \tag{3.30}$$

Elimination of $k$ in Eqn. 3.29 and Eqn. 3.30 results in

$$E(\alpha_1) = \frac{v_1}{1-\frac{v_2}{v_1}+v_1-v_2} \tag{3.31}$$

for the estimation of the global relative error.

In the case that $C(t;\alpha)$ is a monotonic decreasing function with respect to $\alpha$ for all $t$ as

$$\forall t\ (\alpha_1 < \alpha_2 \rightarrow C(t;\alpha_1) > C(t;\alpha_2))$$

the errors are expressed by

$$V_r(\alpha) = \frac{P(\alpha)-P(\alpha+\Delta)}{P(\alpha)} \tag{3.32}$$

$$E(\alpha) = \frac{P(\alpha)-P_\infty}{P_\infty} \tag{3.33}$$

resulting in $E(\alpha_1)$ as

$$E(\alpha_1) = \frac{v_1}{1 - \frac{v_2}{v_1} - v_1 + v_2} \tag{3.34}$$

Supposing that $v_2 = 1/2v_1$ and $v_1 \ll 1$, the global error $E(\alpha)$ could be estimated to be the double of the local error $V_r(\alpha)$.

## 3.3 Concluding remarks

A compartment model is constructed to represent the chemical transmission process of ACh at the neuromuscular junction as an RD system in a two-dimensional space of axis-symmetrical disc of the synaptic cleft for generation of the MEPC. The model might be regarded as the two-dimensional extension of the RD system models proposed previously [7, 26, 32], which essentially behave as one-dimensional compartment models because the diffusion process in either of two directions is simplified, so that these models are represented as the special case of one compartment for either the transverse or radial diffusion process in the two-dimensional compartment model.

The evaluation of the optimal values for the parameters of the compartment model reveals that the model with $L \geq 500$nm, $N_t \geq 1$ and $N_r \geq 10$ sufficiently represents the dynamic behavior of the RD system for the chemical transmission process in the two-dimensional space of the synaptic cleft without the junctional fold. The finding of $N_t \geq 1$ implies that the homogeneous state is possible in the transverse direction, so that the model proposed by Wathey [32] might be appropriate for modeling of generation of the MEPC at the synapse without the junctional fold. It should be noted that $N_r \geq 10$ does not mean the requirement of at least ten compartments in the radial direction. In fact $N_r$ less than 10 might be possible because of quite small value of $V_r$ ($\leq 1.33\%$) for $N_r = 10$. The minimum ten compartments in the radial direction is due to the method of uniform discretization as in elements of equal size used in this study. The nonuniform discretization would lead to different evaluation of the minimum values for the parameters.

The release mechanisms of ACh from the synaptic vesicle are modeled by expression of the release rate with the parameters of $a$ and $\rho$ in Eqn. 3.2 and of the localization of the release area with the radius of $d$. Though it is natural that $d$ is set to be the same as $\rho$, that requires so many number of compartments, demanding the huge computational cost or the nonuniform discretization. In the model the junctional fold is simplified as a concentric cylinder with its top surface attached to the bottom of the disc so as to open a hole to the synaptic cleft at the postsynaptic membrane. Inclusion of the shape of gutter needs three-dimensional modeling of the space, which increases the computational costs.

# Chapter 4

# Characterization of the Mechanisms in the Transmission Process

The dynamic behavior of the RD system for ACh is characterized with its parameters, such as kinetic parameters for the reactions in the cleft, diffusion coefficient of ACh in the cleft, facilitation factors for release mechanisms of ACh and structural parameters of the synaptic cleft. In this chapter the compartment model constructed in the preceding chapter is applied to examination for the effects of the diffusion coefficient of ACh and the release mechanisms on generation of the MEPC at the neuromuscular junction. The simulations are performed under the various values of these parameters to lead to the quantitative characterization of the dynamic behavior of the RD system with estimation of the suitable values of the parameters for the reproduction of the empirical MEPC. It is justifiably assumed in the simulation that the variation in concentration of the open channel form of AChR in response to a quantal release of ACh corresponds to transient evolution of the MEPC.

The behavior of the RD system for ACh is naturally dependent on the value of diffusion coefficient of ACh. Though it is difficult to experimentally measure the diffusion coefficient of ACh in the cleft, a rational evaluation is possible by simulation of the compartment model with various values of $D_t$ and $D_r$. The simulation analysis of the RD system reveals that the radial diffusion process of ACh has more distinctive effects on generation of the MEPC than the transverse process. In fact, the anisotropic diffusion is effective in the RD system since the diffusion coefficient of ACh in the radial direction is evaluated to be about $1.0 \times 10^{-6}\mathrm{cm}^2\mathrm{sec}^{-1}$ for appropriate characterization of the MEPC, on which the diffusion coefficient in the transverse direction larger than $2.0 \times 10^{-6}\mathrm{cm}^2\mathrm{sec}^{-1}$ virtually has no effects.

The compartment model is also applied for evaluating quantitatively the feasibility of the expanding pore mechanism and the active release mechanism in the generation of MEPC at the neuromuscular junction. In the model the ACh release mechanisms are formulated as an additional differential equation with the respective parameters of the pore expanding rate for the expanding pore mechanism and of the acceleration rate for the active release mechanism. The responses with the various parameters of the ACh release mechanisms are compared with the empirical data of MEPC for evaluating the characteristic parameters in the release mechanisms. In the expanding pore mechanism the expanding rate of the pore more than 10nm/msec and the diffusion coefficient of ACh in the synaptic cleft ($D_r$) of about $1.0 \times 10^{-6}\mathrm{cm}^2\mathrm{sec}^{-1}$ yield the amplitude, the growth time and the decay constant of the MEPC in agreement with the empirical data. In the active release mechanism 10-fold acceleration of the natural diffusion and a similar value of $D_r$ are required to suit for the empirical MEPC.

## 4.1 Diffusion process of ACh in the synaptic cleft

### 1. Isotropic diffusion of ACh

The compartment model constructed by optimal selection of the critical radius and the numbers of compartments is applied to examination of the effects of the diffusion coefficient of ACh on generation of the MEPC with respect to the feasibility of the compartment model and the estimation of the value of the diffusion coefficient of ACh suitable for the empirical MEPC. The two-dimensional compartment model with the parameters of $L =$ 500nm, $N_r = 10$, $N_t = 3$, $F_w = 0$ (foldless), and $a = \infty$ (instantaneous release mechanism of ACh) is employed for the simulation. Though $N_t = 1$ represents the minimum model, three compartments in the transverse direction are assigned to the basic processes of the chemical transmission, that is, the release of ACh, the diffusion in the cleft and the hydrolysis by AChE, and the interaction with AChR for the MEPC generation, since the analysis of the behavior in each compartment may characterize the respective basic processes.

The simulation of the responses is performed with concomitant variation in the diffusion coefficients for the transverse and radial diffusion processes, that is, for the case of isotropic diffusion in the disc with $D_t = D_r$ (denoted as $D$). The response of $C(t)$ varies according to

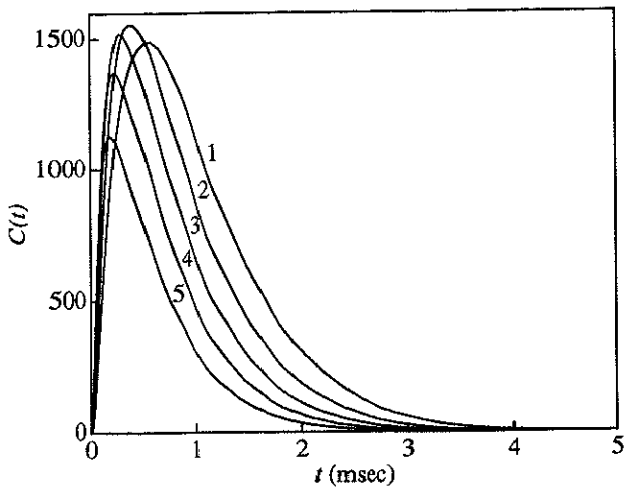


**Fig.4.1.** Effect of the diffusion coefficient of ACh on the response of the total number of the open channel form of AChR. The number on a curve corresponds to the value of $D$ (in $10^{-6}\text{cm}^2\text{sec}^{-1}$): 1: 0.25, 2: 0.5, 3: 1.0, 4: 2.0, and 5: 4.0. The unit of $C(t)$ on the ordinate is the number of the open channel form of AChR.

**Table 4.1** Variation of the characteristic parameters of the MEPC with the diffusion coefficients

| $D$ ($\times 10^{-6}$cm$^2$sec$^{-1}$) | $C_{max}$ (number) | $t_m$ ($\mu$sec) | $\tau$ (msec) |
|---|---|---|---|
| 0.25 | 1478 | 202 | 1.10 |
| 0.50 | 1553 | 143 | 0.97 |
| 1.00 | 1517 | 105 | 0.91 |
| 2.00 | 1373 | 81 | 0.79 |
| 4.00 | 1126 | 65 | 0.72 |

various values of the diffusion coefficient as shown in Fig. 4.1. The maximum concentration (peak) is attained around 0.5msec after the release of ACh, and all the channels close within about 4msec. The larger diffusion coefficient decreases the times taken to attain the peak and to fall from the peak to almost null concentration, and makes the response steeper. The highest peak of $C(t)$ is observed at $D = 0.5 \times 10^{-6}$cm$^2$ sec$^{-1}$. The characteristic values of $C(t)$ for each of the diffusion coefficients are demonstrated in Table 4.1. It is thus revealed that the diffusion coefficient around $1.0 \times 10^{-6}$cm$^2$sec$^{-1}$ yields these characteristic values which are in good agreement with the empirical $C_{max}$ value of 1500 described in Section 2.2.

The temporal change in radial distribution of ACh concentration in the middle com-

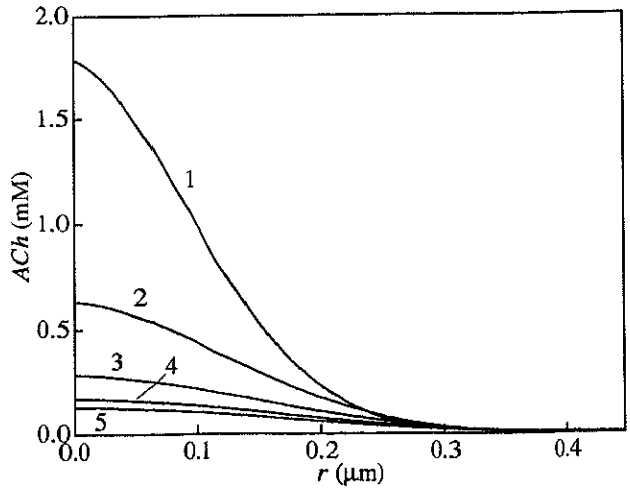


**Fig.4.2.** Temporal change in the radial distribution of ACh concentration at the middle compartment on the transverse coordinate. The number on a curve indicates the time in $10^{-1}$msec.

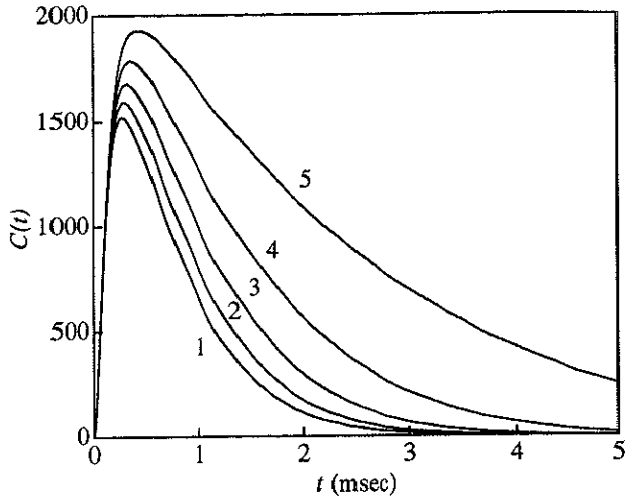


**Fig.4.3.** Effect of the AChE activity on the response of the total number of the open channel form of AChR. The number on a curve corresponds to the relative AChE activity : 1: 1.0, 2: 0.75, 3: 0.50, 4: 0.25, and 5: 0.0. The unit of $C(t)$ on the ordinate is the number of the open channel form of AChR.

partment on the transverse coordinate is displayed in Fig. 4.2 for the system with $D = 1.0 \times 10^{-6}\text{cm}^2\text{sec}^{-1}$, where a substantial gradient in concentration is formed after the release and the peak decreases to about 10% in 0.5msec. The behavior is almost identical in other two compartments. Moreover, increase in the diffusion rate results in steeper concentration gradient and quicker fall of the lower peak.

Furthermore, the effects of inhibition of AChE on the response characteristics have been reported [7, 14], disclosing that the transmission process is also affected severely by the activity of AChE. The behavior of the model with $D = 1.0 \times 10^{-6}\text{cm}^2\text{sec}^{-1}$ is examined with variation in the density of AChE in the disc. As seen in Fig. 4.3, the more inhibition of AChE (i.e., less density of AChE) makes the peak of $C(t)$ higher and the falling curve shallower. The characteristic values obtained as in Table 4.2 indicate good agreement with the empirical observation of the effects of AChE inhibition that the amplitude $C_{max}$ gets higher by a factor of 1.3 and the growth time $t_m$ increases by a factor of 1.4, while the decay constant $\tau$ elongates by a factor of 3. It is thus inferred that the basic processes in the chemical transmission are appropriately represented by this RD system in the disc.

Table 4.2 Variation of the characteristic parameters of the MEPC with the AChE activity

| AChE activity (relative) | $C_{max}$(relative) | $t_m$ ($\mu$sec) | $\tau$ (msec) |
|---|---|---|---|
| 1.00 | 1.00 | 105 | 0.86 |
| 0.75 | 1.05 | 111 | 1.00 |
| 0.50 | 1.10 | 117 | 1.18 |
| 0.25 | 1.18 | 127 | 1.56 |
| 0.00 | 1.27 | 141 | 2.63 |

Diffusion coefficient: $D = 1.0 \times 10^{-6}\text{cm}^2\text{sec}^{-1}$

**2. Anisotropic diffusion of ACh**

Introduction of the anisotropic diffusion into the transverse and radial directions would further reveal the effects of diffusion rates on the characteristic behavior of the MEPC. The simulation with individual variation in $D_t$ and $D_r$ between 0.25 and 4.0 (in $10^{-6}\text{cm}^2\text{sec}^{-1}$) is performed to examine these effects. Figure 4.4(a) illustrates the effect on the amplitude $C_{max}$, which gets higher with increase of $D_t$ in its variation range and $D_r$ up to $0.5 \times 10^{-6}\text{cm}^2\text{sec}^{-1}$, while increase in $D_r$ above $0.5 \times 10^{-6}\text{cm}^2\text{sec}^{-1}$ reduces $C_{max}$ against the opposite effect by $D_t$. It is noted that the effect of $D_r$ is more substantial than that of $D_t$, which is still enhanced at larger $D_r$. As seen in Fig. 4.4(b), the growth time $t_m$ decreases sharply as $D_r$ increases, thus making $C(t)$ reach the maximum more quickly. $D_t$ has little effect on $t_m$ in its variation range, especially with $D_r$ less than $1.0 \times 10^{-6}\text{cm}^2\text{sec}^{-1}$, indicating that the radial diffusion mainly determines the growth time. Figure 4.4(c) displays the effect on the decay constant $\tau$, which decreases with larger $D_r$ to cause more rapid descent of $C(t)$ from the peak. The effect of increase in $D_t$, which is weaker than that in $D_r$, also tends to result in smaller $\tau$.

It is thus revealed from the analysis of the effects of diffusion rates in this compartment model that the radial diffusion process has more distinctive effects on generation of the MEPC than the transverse one and that the radial diffusion with $D_r$ around $1.0 \times 10^{-6}\text{cm}^2\text{sec}^{-1}$ appropriately yields the characteristics of the transmission process without significant effects of the transverse diffusion with $D_t$ larger than $2.0 \times 10^{-6}\text{cm}^2\text{sec}^{-1}$. In conclusion, the anisotropic compartment model with $L = 500\text{nm}$, $N_r = 10$ and $N_t = 3$ in the two-dimensional space of

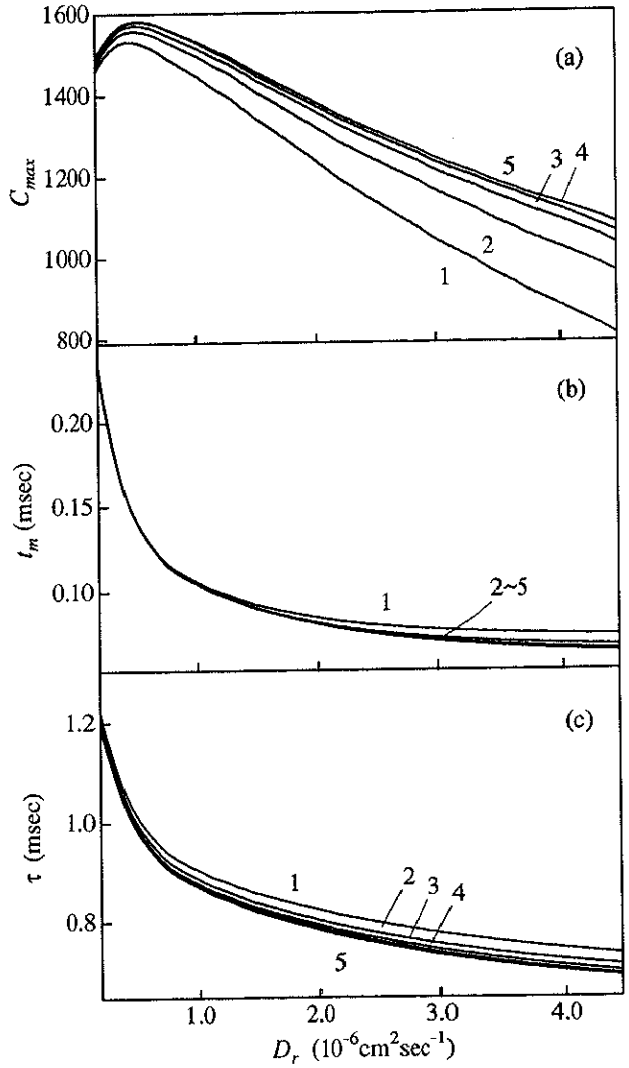


**Fig.4.4.** Effects of the radial diffusion coefficient on the response of the total number of the open channel form of AChR. Effects on: (a) the amplitude, (b) the growth time, (c) the decay constant. The number on a curve corresponds to the value of $D_t$ (in $10^{-6}$cm$^2$sec$^{-1}$): 1: 0.25, 2: 0.5, 3: 1.0, 4: 2.0, 5: 4.0. The unit of $C_{max}$ on the ordinate is the number of the open channel form of AChR.

axis-symmetrical disc of the synaptic cleft suitably represents the generation of MEPC at the neuromuscular junction.

## 4.2 Mechanisms for neurotransmitter release from the synaptic vesicle

### 1. Expanding pore mechanism

The process of neurotransmitter release at the neuromuscular junction needs to be represented appropriately in modeling of the synaptic chemical transmission as an RD system. As shown in Fig. 3.1, the compartment model constructed takes the release mechanism of the expanding pore into consideration. The computer simulation is performed for analysis of the behavior of the model with respect to the effects of the characteristic parameter in the mechanism on generation of the MEPC. The compartment model with the parameters of $L = 500\text{nm}$, $N_r = 10$, $N_t = 1$ and $F_w = 0$ (foldless) is chosen for the simulation. Assumption of the homogeneous distribution of ACh in the transverse direction ($N_t = 1$) is justified with the results of the dynamic behavior of ACh in Section 3.1. This also leads to reduction in the dimension of the model.

Though $D = 1.0 \times 10^{-6}\text{cm}^2\text{sec}^{-1}$ is proposed as the appropriate value for the isotropic diffusion in the preceding section, the accurate value is still unknown, so that the simulation analysis is performed in the range of $(0.5 \sim 4.0) \times 10^{-6}\text{cm}^2\text{sec}^{-1}$ for $D_r$ in order to examine the effects of the radial diffusion on the release mechanism. The parameter of $D_t$ is not required in this analysis because of the assumption of homogeneous distribution of ACh in the transverse direction in the cleft. $D_p$ is set to the same value of $D_r$. The effects of the expanding pore is examined on the behavior of $C(t)$ (i.e., equivalent of the MEPC) by variation in the values of the expanding rate ($0 \leq b \leq 25\text{nm/msec}$). The values of the other parameters used are as given in Section 3.1.

The responses of $C(t)$ to a quantal release of ACh are demonstrated in Fig. 4.5. The release by natural diffusion through the fixed radius pore ($b = 0$) yields the curve of number 1 in solid line, indicating that the peak of $C(t)$ significantly decreases, and the times taken to attain the peak and to fall to almost null concentration increase, compared with the curve in dotted line corresponding to the instantaneous spread. The higher expanding rate of the pore makes the response quicker, resulting in the curve similar to the instantaneous spread in the case of $b = 25$ nm/msec. It is noted that the ACh concentration in the synaptic

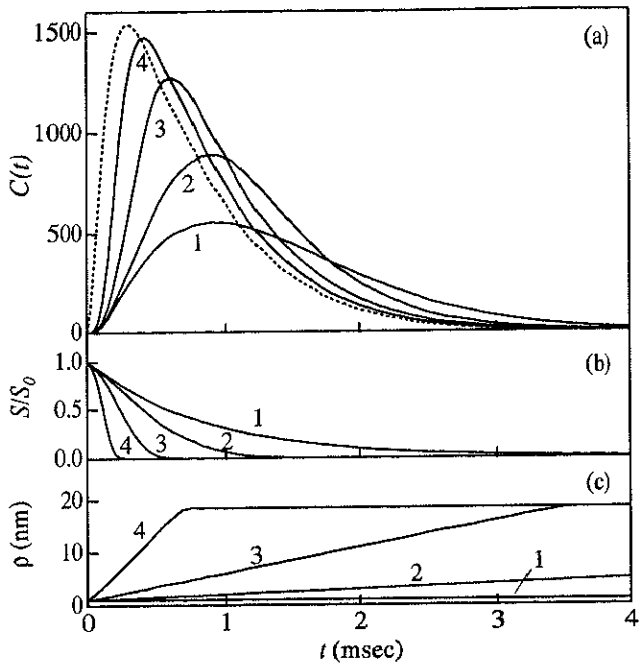


**Fig.4.5.** Effect of the pore expanding rate on the response. Time courses of: (a) $C(t)$, (b) the ratio of $S(t)$ to $S_0$ (the initial consentration of ACh in the synaptic vesicle), (c) expansion of the radius $\rho$ of the pore. The number on a solid curve corresponds to the value of $b$ (in nm/msec): 1: 0.0, 2: 1.0, 3: 5.0, and 4: 25.0. The dotted curve indicates $C(t)$ for the instantaneous spread of ACh. The unit of $C(t)$ is the number of the open channel form of AChR.

vesicle $S(t)$ decreases to the almost null concentration at the time when $C(t)$ attains the peak except for the case of no expansion ($b = 0$) and that the time taken to empty the vesicle is less than the time for expansion of $\rho$ to the maximum. This implies that the upper limit of $\rho(t)$ might not be required for the model with the parameters adopted.

The effects of the expanding rate of the pore in the range of $0.025 \leq b \leq 100$ (nm/msec) on the characteristic parameters ($C_{max}$, $t_m$ and $\tau$) with variation of the diffusion coefficients $D_r$ ($= D_p$) in the range of 0.5 to 4.0 (in $10^{-6}\text{cm}^2\text{sec}^{-1}$) are demonstrated in Fig. 4.6. The change of the expanding rate in the range of $0.1 \leq b \leq 10$ (nm/msec) has significant effects on $C(t)$. The quicker expansion makes the amplitude $C_{max}$ higher and the decay constant $\tau$ lower. On the other hand, the effect on the growth time $t_m$ is varied. In the case of $D_r = 0.5$ or 1.0 ($\times 10^{-6}$ $\text{cm}^2\text{sec}^{-1}$) the larger expanding rate up to the value of $b$ about 0.5 increases $t_m$, and then decreases it in the still larger value of $b$. On the contrary, the value of $t_m$

monotonously decreases in the case of $D_r = 2.0$ or 4.0 ($\times 10^{-6}$cm$^2$sec$^{-1}$). The effects of the expanding rate on the characteristic values saturate in the range of $b$ over 10nm/msec. It is also noticed that the change in $b$ has the larger effects on the characteristic values with the smaller diffusion coefficients.

It follows from Fig. 4.6(a) that the release mechanism of ACh with the slow expanding rate of the pore less than about 10nm/msec including the natural diffusion through the fixed-size pore ($b = 0$) cannot suffice the empirical data of the amplitude $C_{max}$ (= 1500, as

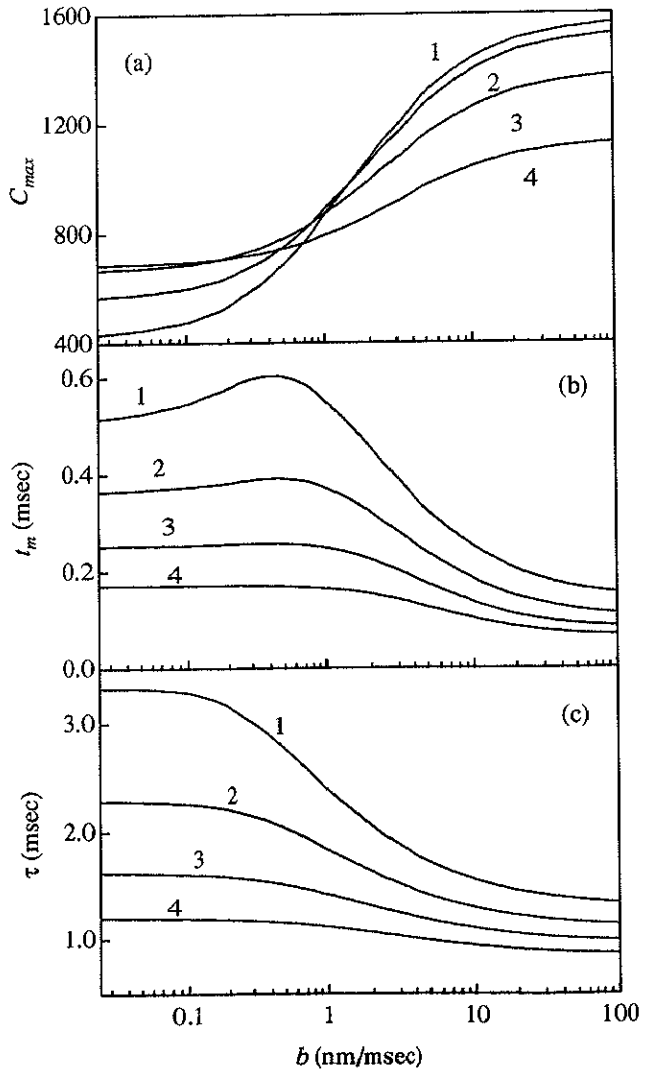


**Fig.4.6.** Effects of the pore expanding rate on the response of the total number of the open channel form of AChR. Effects on: (a) the amplitude, (b) the growth time, (c) the decay constant. The number on a curve corresponds to the value of $D_r(= D_p)$ (in $10^{-6}$cm$^2$sec$^{-1}$): 1: 0.5, 2: 1.0, 3: 2.0, and 4: 4.0. The unit of $C(t)$ on the ordinate is the number of the open channel form of AChR.

mentioned in Section 2.2) because the value is too low for the MEPC. The expanding rate $b$ more than 10nm/msec with $D_r = 0.5$ or 1.0 ($\times 10^{-6}$cm$^2$sec$^{-1}$) could yield the empirical MEPC, while with $D_r = 2.0$ or 4.0 ($\times 10^{-6}$cm$^2$ sec$^{-1}$) the amplitude $C_{max}$ is too low for the empirical data.

In conclusion, the expanding pore mechanism could reproduce the empirical MEPC with the expanding rate $b$ of about 10nm/msec and with the diffusion coefficient $D_r$ ($= D_p$) around $1.0 \times 10^{-6}$cm$^2$sec$^{-1}$.

**2. Active release mechanism**

The feasibility of the active release mechanism such as an active transport coupled with ion exchange is examined by the similar simulation with the same RD system. The active release mechanism is represented with the acceleration coefficient $a$ in Eqn. 3.2 for the ACh influx into the synaptic cleft. The simulation for the acceleration of the ACh influx rate in the range of $1 \leq a \leq 100$, that is, $a$-fold rate of the natural diffusion through the fixed-size pore of $b_0$ is performed with variation of the diffusion coefficients $D_r$ ($= D_p$) between 0.5 and 4.0 (in $10^{-6}$cm$^2$sec$^{-1}$).

The change of the acceleration rate in the range less than 10-fold has significant effect on all of the characteristic parameters in $C(t)$ as shown in Fig. 4.7. The quicker release makes the amplitude $C_{max}$ higher and the growth time $t_m$ and the decay constant $\tau$ lower. The effects of the acceleration rate on the characteristic values saturate in the range of $a$ over 10. It is also noticed that the change in $a$ has the larger effects on the characteristic values with the smaller diffusion coefficients, similarly to the effects of the expanding rate. It is revealed that the acceleration rate more than 10-fold with $D_r = 0.5$ or 1.0 ($\times 10^{-6}$cm$^2$sec$^{-1}$) could yield the MEPC characterized with the known values of $C_{max}$, $t_m$, and $\tau$ given in Section 2.2, while with $D_r = 2.0$ or 4.0 ($\times 10^{-6}$cm$^2$ sec$^{-1}$) the amplitude $C_{max}$ is too low for the empirical data.

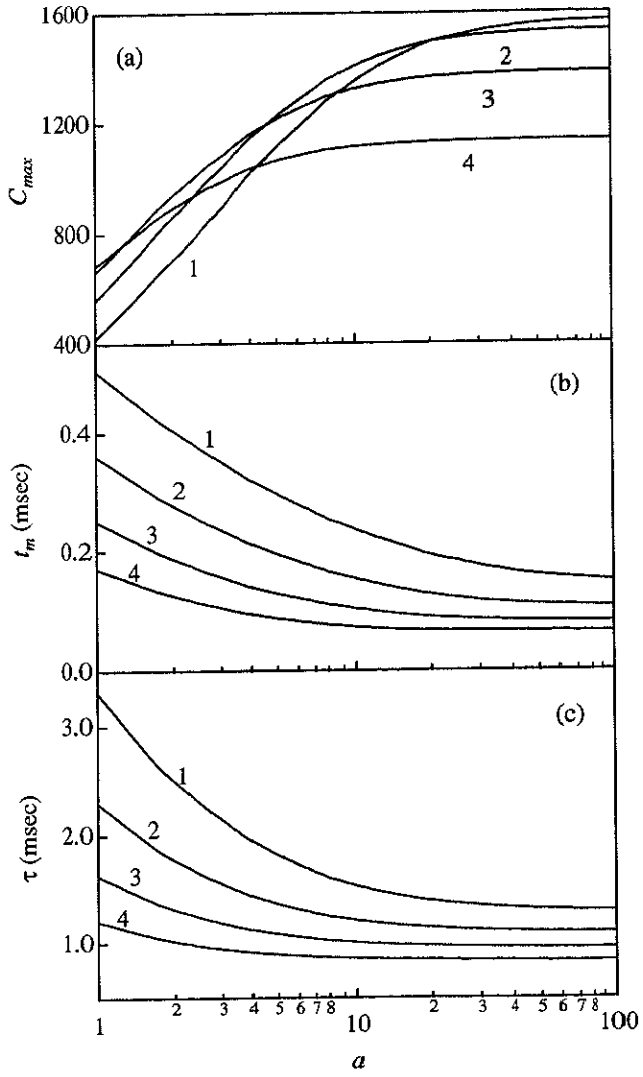


**Fig.4.7.** Effects of the acceleration rate of the ACh release on the response of the total number of the open channel form of AChR. Effects on: (a) the amplitude, (b) the growth time, (c) the decay constant. The number on a curve corresponds to the value of $D_r(= D_p)$ (in $10^{-6}\text{cm}^2\text{sec}^{-1}$): 1: 0.5, 2: 1.0, 3: 2.0, and 4: 4.0. The unit of $C(t)$ on the ordinate is the number of the open channel form of AChR.

In conclusion, the active release mechanism could reproduce the empirical MEPC with the acceleration rate 10 times of the natural diffusion and with the diffusion coefficient $D_r$ of 0.5 or 1.0 ($\times 10^{-6}\text{cm}^2\text{sec}^{-1}$).

## 4.3 Concluding remarks

The model for the simulation analysis in this study might be regarded as the two-dimensional extension of the similar models proposed previously [7, 26, 32], which essentially behave as one-dimensional compartment models because the diffusion process in either of two directions is simplified. The Friboulet's model [7] in which the radial diffusion undergoes simple efflux of ACh due to concentration gradient, is not satisfactory now that the radial diffusion is revealed to have distinctive effects on the dynamic behavior of the RD system for ACh [23]. The models with homogeneity in the transverse direction [26, 32] would be reasonable for $D_t$ larger than $2.0 \times 10^{-6}\mathrm{cm}^2\mathrm{sec}^{-1}$, but the transverse diffusion has also to be taken into consideration for probable case of $D_t$ smaller than $2.0 \times 10^{-6}\mathrm{cm}^2\mathrm{sec}^{-1}$.

For the RD system with isotropic diffusion (i.e., $D_t = D_r$) assumed, the diffusion coefficient of ACh in the disc is evaluated to be about $1.0 \times 10^{-6}\mathrm{cm}^2\mathrm{sec}^{-1}$, with which the simulation yields the behavior of a typical MEPC characterized by the parameters in quantitative agreement with those from the empirical analysis. It is further demonstrated with independent variation in $D_t$ and $D_r$ that the radial diffusion has more distinctive effects than the transverse diffusion, that is, in the RD system with anisotropic diffusion, increase in $D_r$ significantly reduces all of $C_{max}$, $t_m$ and $\tau$. Moreover, the effects of $D_t$ are still less discernible at smaller $D_r$.

It should be noted that the transverse and radial diffusion processes have the opposite effects on $C_{max}$, resulting in the maximum in $C_{max}$ with $D_r$ of about $0.5 \times 10^{-6}\mathrm{cm}^2\mathrm{sec}^{-1}$. Increase in $D_r$ with larger $D_t$ reduces $C_{max}$, and also makes the shape of $C(t)$ sharper because the radial diffusion plays an important role in conversion from AChR doubly bound with ACh to AChR singly bound with ACh. Higher $C_{max}$ and sharper peak are suitable for generation of the MEPC, while efficient generation of whole endplate current by summation of the MEPCs needs some width in the peak of MEPC due to slight delay in release from each of the engaged vesicles.

The compartment model is also applicable to the analysis of neurotransmitter release mechanisms in generation of the MEPC. The simulation analysis reveals that the natural diffusion through a pore of a fixed radius of 1.0nm, which is evaluated as the initial radius

[12, 29, 30], is not sufficient for reproduction of the empirical data. The amplitude $C_{max}$ of the MEPC less than half of the known value is yielded by the model regardless of the values of diffusion coefficient of ACh. The times characteristic to the peak are too long again compared with the known values of $t_m$ and $\tau$ [7]. Although the growth time $t_m$ would be acceptable for the diffusion coefficients greater than $2.0 \times 10^{-6}\text{cm}^2\text{sec}^{-1}$ with respect to the data by Van der Kloot [30], $C_{max}$ is too low to agree with the empirical data. Therefore, some mechanism additional to the natural diffusion through the fixed-size pore is required for the model to appropriately represent the generation of MEPC.

The mechanism of the expanding pore thus is examined to reveal that it could reproduce the empirical MEPC with the expanding rate more than 10nm/msec and with the diffusion coefficient $D_r$ $(= D_p)$ of 0.5 or 1.0 $(\times 10^{-6}\text{cm}^2\text{sec}^{-1})$. This would be in good agreement with the results of Stiles [29] that the mechanism with the expanding rate of 25nm/msec generates the behavior like the empirical MEPC. On the other hand, the mechanism of slow expanding at 0.4nm/msec is found to be unsatisfactory [12]. The behavior of the acceleration mechanism for the release of ACh proposed by Khanin *et al.* [12] is also analyzed with the compartment model. The mechanism is found to work satisfactorily with the acceleration rate 10 times of the natural diffusion and with the diffusion coefficient $D_r$ of 0.5 or 1.0 $(\times 10^{-6}$ cm $^2\text{sec}^{-1})$.

It follows that the assumption of instantaneous spread of ACh in the synaptic cleft, which has been widely employed to simplify modeling, could be regarded as an extreme case of the large value of the expanding rate $b$ or the acceleration parameter $a$. The amplitude $C_{max}$ approaches up to that for the case of instantaneous spread, while the growth time $t_m$ and the decay constant $\tau$ of the falling phase of $C(t)$ decrease to the corresponding characteristic values. Therefore, if the rapid expanding pore or the acceleration of release of ACh should be the actual mechanism, the model with the instantaneous spread would overestimate the amplitude, and underestimate the growth time and the decay constant of the MEPC.

The differentiation of the anisotropic effects is apparently due to the size and shape of the disc of the synaptic cleft for the model. The structure of the cleft is crucial to the chemical transmission process. Variation in thickness of the cleft and the actual shape in

three-dimensional space should be taken into account for modeling and analysis. Extension of the two-dimensional compartment model to a three-dimensional model is required for full elucidation of the chemical transmission process. For the analysis it is interesting to examine whether formulation with the Michaelis equations for AChE and AChR are valid in this two-dimensional RD system. The validity of the Michaelis equation is verified for a simple Michaelis-Menten-type reaction in uniform distribution in one-dimensional space [22]. It is further of interest to evaluate the relationship of $D_t$ and $D_r$ with the distribution of constituent materials in the cleft.

# Chapter 5

# Effects of the Specific Structures on the Transmission Process

The biochemical systems have been developed through the long lasting evolution process, implying that sorts of quantitative optimization might have been accomplished with respect to the parameters associated with the functions of the systems. Hence, the parameters in the chemical transmission process would be optimal with respect to the generation of MEPC. The significance of the specific structure of the junctional folds and the quantal release of neurotransmitter at the neuromuscular junction might thus be elucidated by examination of the effects of the structural parameters, such as the width and the depth of the junctional folds and the size of the localized release area of ACh as a result of the quantal release from synaptic vesicles, on generation of the MEPC.

The two-dimensional compartment model is applied to analyze the dynamic behavior of ACh in the synaptic cleft with a junctional fold, demonstrating that the existence of the junctional fold causes the substantial effects on generation of the MEPC at the neuromuscular junction. Attachment of the cylinder of 50nm radius to the disc results in higher amplitude of the MEPC, steeper rise and slower fall of the peak. The larger radius of the hole (100nm) makes the amplitude lower than the foldless case regardless of the values of the diffusion coefficient. The higher value of the amplitude for 50nm radius of the cylinder than those for 100nm radius and foldless case indicates that the maximal amplitude of the MEPC may be attained with an optimal width of the junctional fold. The depth of the fold has less distinctive effect on the MEPC than the radius.

For further application, the simulation analysis is performed with the compartment model

to clarify the biochemical significance of the quantal release mechanism of ACh with respect to generation of the MEPC. It is revealed that the mechanism raises the amplitude of MEPC significantly. The evaluation of the size of the release area of ACh is further attempted with regard to the EPC responding to arrival of the action potential at the nerve terminal. The same effect of the quantal release mechanism is again assured in the case of EPC. The localized release of ACh makes the amplitude of EPC higher by a factor about 2 compared with that in the homogeneous release of ACh, implying that the quantal release mechanism works as an amplifier of the EPC with the fixed amount of ACh available.

## 5.1 Effects of the junctional folds

The junctional folds with some specific structure exist on the postsynaptic membrane at the neuromuscular junction as described in Section 2.1. Though the effect of the junctional fold on generation of the MEPC is analyzed with a one-dimensional compartment model in the transverse direction [7], the conclusion that the existence of the folds reduces the amplitude of the MEPC significantly is not reliable because the model simplifies the radial diffusion process of ACh in the cleft which has the significant effects on generation of the MEPC as clarified in Section 4.1. While in the one-dimensional model the attachment of a fold is obliged to be treated as the change of the width of the cleft, the two-dimensional compartment model includes the structure of the fold as the concentric cylinder with the radius of $F_w$ and the height of $F_d$ attached on the bottom of the disc.

The simulation analysis is performed to examine the effects of the junctional folds on the behavior of $C(t)$ (i.e., equivalent of the MEPC) by variation in the values of the radius ($F_w$ = 0, 50nm, and 100nm) and the height ($F_d$ = 500nm and 1000nm) of the cylinder. The two-dimensional compartment model with the parameters of $L$ = 500nm, $N_r$ = 10, $N_t$ = 3, $a = \infty$ (instantaneous release mechanism of ACh) and the isotropic diffusion of ACh ($D_r = D_t [= D]$) is employed for the simulation. The analysis is carried out in the range of $D$ between $(0.25 \sim 4.0) \times 10^{-6}\text{cm}^2\text{sec}^{-1}$ and the values of the other parameters used are as described in Section 3.1.

The responses of $C(t)$ to a quantal release of ACh are demonstrated in Fig. 5.1. The maximum concentration (peak) is attained around 0.5msec after the release of ACh, and all the channels close within about 4msec. The curve of $C(t)$ with $F_w$ = 50nm always locates over the curve for the foldless case, which in turn is always above the curve with $F_w$ = 100nm, regardless of the values of the diffusion coefficient $D$.

As the responses are characterized quantitatively with the amplitude $C_{max}$, growth time $t_m$ and decay constant $\tau$ in this study, the effects of the junctional fold and the diffusion coefficient on the characteristic parameters are presented in Table 5.1. Attachment of the cylinder with $F_w$ = 50nm to the disc results in about 5% higher $C_{max}$, steeper rise and slower fall of the peak compared with the foldless case for whole the range of the diffusion

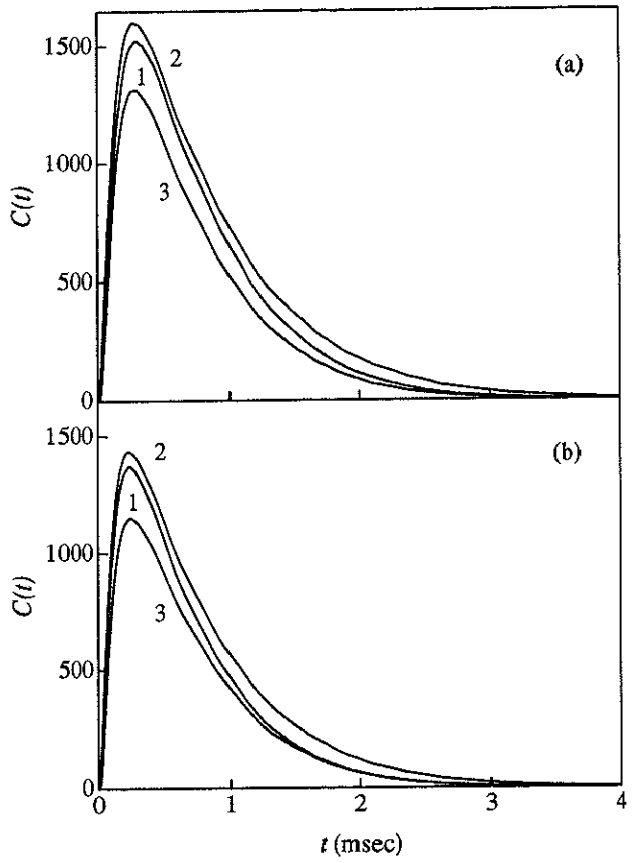


**Fig.5.1.** Effects of the radius of the junctional fold on the response of the total number of the open channel form of AChR. Duffusion coefficient $D$ (in $10^{-6}\text{cm}^2\text{sec}^{-1}$): (a) 1.0, (b) 2.0. The number on a curve corresponds to the value of the radius $F_w$ (in nm): 1: 0, 2: 50, and 3: 100. The unit of $C(t)$ on the ordinate is the number of the open channel form of AChR.

coefficient examined. The larger radius of the cylinder ($F_w = 100\text{nm}$) makes the amplitude $C_{max}$ around 15% lower than the foldless case regardless of the values of $D$, while the effects of $F_w$ on the growth time $t_m$ and the decay constant $\tau$ are dependent on the value of $D$. For $D$ less than $2.0 \times 10^{-6}\text{cm}^2\text{sec}^{-1}$ the larger radius of the cylinder makes $t_m$ lower and $\tau$ higher, while for $D$ more than $2.0 \times 10^{-6}\text{cm}^2\text{sec}^{-1}$ the opposite effects arise. The higher value of $C_{max}$ with $F_w = 50\text{nm}$ than with $F_w = 100\text{nm}$ and 0 (foldless) indicates that the maximal amplitude of the MEPC may be attained with an optimal width of the junctional fold. It is also found that the depth of the fold has less distinctive effects on $C(t)$ than the radius, and that the junctional folds do not affect the effects of the diffusion coefficients on the response of $C(t)$ such that increase in $D$ reduces all of $C_{max}$, $t_m$, and $\tau$.

**Table 5.1** Effects of the junctional fold on the characteristic parameters of the MEPC

| $w_f$ (nm) | $d_f$ (nm) | $D$ ($\times 10^{-6}$cm$^2$sec$^{-1}$) | $C_{max}$ | | $t_m$ ($\mu$sec) | | $\tau$ (msec) | |
|---|---|---|---|---|---|---|---|---|
| | foldless | 0.25 | 1490 | (1.00) | 205 | (1.00) | 1.16 | (1.00) |
| | | 0.50 | 1560 | (1.00) | 144 | (1.00) | 1.00 | (1.00) |
| | | 1.00 | 1520 | (1.00) | 105 | (1.00) | 0.89 | (1.00) |
| | | 2.00 | 1370 | (1.00) | 81 | (1.00) | 0.79 | (1.00) |
| | | 4.00 | 1130 | (1.00) | 65 | (1.00) | 0.70 | (1.00) |
| 50 | 500 | 0.25 | 1620 | (1.09) | 168 | (0.82) | 1.20 | (1.03) |
| | | 0.50 | 1660 | (1.07) | 124 | (0.86) | 1.05 | (1.05) |
| | | 1.00 | 1600 | (1.05) | 94 | (0.90) | 0.95 | (1.07) |
| | | 2.00 | 1440 | (1.05) | 76 | (0.94) | 0.89 | (1.13) |
| | | 4.00 | 1190 | (1.05) | 65 | (0.99) | 0.81 | (1.16) |
| | 1000 | 0.25 | 1620 | (1.09) | 168 | (0.82) | 1.20 | (1.03) |
| | | 0.50 | 1660 | (1.07) | 124 | (0.86) | 1.04 | (1.04) |
| | | 1.00 | 1560 | (1.05) | 94 | (0.90) | 0.93 | (1.05) |
| | | 2.00 | 1430 | (1.04) | 75 | (0.93) | 0.84 | (1.06) |
| | | 4.00 | 1170 | (1.04) | 63 | (0.97) | 0.77 | (1.10) |
| 100 | 500 | 0.25 | 1370 | (0.92) | 147 | (0.72) | 1.00 | (0.86) |
| | | 0.50 | 1390 | (0.90) | 113 | (0.79) | 0.89 | (0.89) |
| | | 1.00 | 1320 | (0.87) | 91 | (0.87) | 0.84 | (0.94) |
| | | 2.00 | 1150 | (0.84) | 78 | (0.96) | 0.81 | (1.03) |
| | | 4.00 | 930 | (0.83) | 71 | (1.09) | 0.80 | (1.14) |
| | 1000 | 0.25 | 1370 | (0.92) | 147 | (0.78) | 1.00 | (0.86) |
| | | 0.50 | 1390 | (0.90) | 113 | (0.78) | 0.88 | (0.88) |
| | | 1.00 | 1310 | (0.86) | 90 | (0.86) | 0.82 | (0.92) |
| | | 2.00 | 1140 | (0.83) | 76 | (0.94) | 0.77 | (0.97) |
| | | 4.00 | 910 | (0.81) | 67 | (1.03) | 0.72 | (1.03) |

The value in parenthesis indicates the ratio relative to the value in the foldless case with the corresponding diffusion coefficient $D$ (in $10^{-6}$cm$^2$sec$^{-1}$).

In conclusion, it is suggested that the structure of the junctional fold with the appropriate size of the mouth opening to the synaptic cleft has the function to increase the amplitude of the MEPC by about 5%. The appropriate radius of the mouth is around 50nm in the

case that the structure of the fold is represented as the concentric cylinder attached on the bottom of the disc of the synaptic cleft.

## 5.2 Effects of the localized release of ACh due to the synaptic vesicles

### 1. Effect on the miniature endplate current

ACh molecules are released by a unit of quantum through the pore formed by the fusion of a synaptic vesicle with the presynaptic membrane as described in Section 2.2. This release mechanism is relevant to the release rate of ACh into the cleft and to the release area in the cleft. The effects on the release rate of ACh are analyzed in Section 4.2 to evaluate the functional parameters governing the dynamic behavior of the RD system for ACh. In this section the effects on the release area of ACh are examined with respect to the structural aspect in generation of the MEPC. The quantal release mechanism of ACh localizes the ACh release area in the cleft, which is assumed to be a cylindrical space with the radius ($d$), so that the value of $d$ could be considered to represent the localizability of the release area of ACh due to the specific structure of the synaptic vesicles.

The simulation analysis is performed to examine the effects of the localizability of the ACh release area on the behavior of $C(t)$ (i.e., equivalent of the MEPC) by variation in the values of the radius (25nm $\leq d \leq$ 500nm) to reveal the biochemical functions for the structure of the synaptic vesicles at the neuromuscular junction. The compartment model with the parameters of $L$ = 800nm, $N_r$ = 32, $N_t$ = 1, $F_w$ = 0 (foldless), and $a = \infty$ (instantaneous release mechanism of ACh) is chosen for the simulation. The critical radius (800nm) larger than that for the other analysis in this study is necessary to represent the RD system appropriately in the case for the release area examined with the radius of 500nm as the maximum radius. The analysis is carried out in the range of $D_r$ between $(0.5 \sim 4.0) \times 10^{-6}\text{cm}^2\text{sec}^{-1}$ and $D_t$ is not required in this analysis because of the assumption of homogeneous distribution of ACh in the transverse direction in the cleft ($N_t = 1$).

The effects of the radius of the release area in the range of $25 \leq d \leq 500$ (nm) on the characteristic parameters of $C(t)$ are shown in Fig. 5.2. The change in the size of the ACh release area has significant effects on $C(t)$. Regardless of the value of $D_r$, $C_{max}$ holds a high value for the values of $d$ up to about 200nm, and then it decreases rapidly for larger values of $d$. The value of $t_m$ decreases for the values of $d$ up to about 200nm, and then it increases

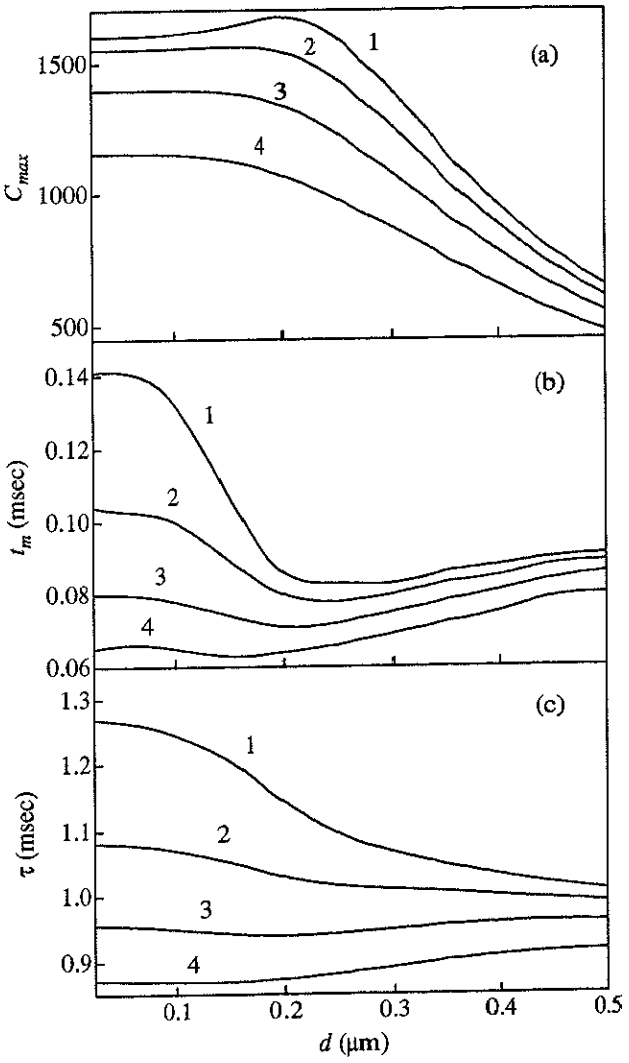


**Fig.5.2.** Effects of the radius $d$ of the ACh release area on the response of the total number of the open channel form of AChR. Effects on: (a) the amplitude, (b) the growth time, (c) the decay constant. The number on a curve corresponds to the value of $D_r$ (in $10^{-6}\text{cm}^2\text{sec}^{-1}$): 1: 0.5, 2: 1.0, 3: 2.0, and 4: 4.0. The unit of $C(t)$ on the ordinate is the number of the open channel form of AChR.

slowly for larger values of $d$. It is also noticed that the value of $t_m$ for $d$ of about 200nm is the lowest. On the other hand, the effect on decay constant $\tau$ is varied. In the case of $D_r = 0.5$ or 1.0 ($\times 10^{-6}$ $\text{cm}^2\text{sec}^{-1}$) the larger radius decreases $\tau$ monotonously. In contrast, the value of $\tau$ monotonously increases in the case of $D_r = 4.0$ ($\times 10^{-6}\text{cm}^2\text{sec}^{-1}$), and remains at almost the same value in the case of $D_r = 2.0$ ($\times 10^{-6}\text{cm}^2\text{sec}^{-1}$). It is also noticed that the change in $d$ has more effects on the characteristic values with the smaller diffusion coefficients. The radius around 200nm seems optimal to produce the sharpest and highest response of $C(t)$.

**Table 5.2** Effect of release area radius on variation of the characteristic parameters of the MEPC with diffusion coefficients

| $D_r$ ($\times 10^{-6}$cm$^2$sec$^{-1}$) | $C_{max}$(relative) | $t_m$ (relative) | $\tau$ (relative) |
|---|---|---|---|
| 0.50 | 2.47 | 1.54 | 1.26 |
| 1.00 | 2.55 | 1.16 | 1.09 |
| 2.00 | 2.54 | 0.93 | 0.99 |
| 4.00 | 2.41 | 0.83 | 0.95 |

"relative": ratios of the value with the release area of 50nm radius to that of 500nm radius

The ratios of every characteristic parameters of $C(t)$ with the localized release area of ACh ($d$ = 50nm) to those with the area of 10-fold radius ($d$ = 500nm) are presented in Table 5.2. It follows in the range of $D_r$ between $(1.0 \sim 4.0) \times 10^{-6}$cm$^2$sec$^{-1}$ that the localizability of the ACh release has significant effects on the amplitude of $C(t)$, while the other characteristic parameters ($t_m$ and $\tau$) are less affected. The amplitude $C_{max}$ produced by the localized release area is about 2.5-fold to that by the release area of the 10-fold radius, while the values of the other parameters are varied by about 10%.

In conclusion, it is suggested that the localization of the release area of ACh has significant effects on generation of the MEPC, especially on the amplitude, which gets higher by a factor about 2.5 compared with that with the large release area.

### 2. Effect on the endplate current

An arrival of the action potential to the nerve terminal induces the release of a few hundred quanta of ACh into the cleft, resulting in depolarization of the muscle cell which is observed as the endplate current (EPC). The EPC could be considered as the sum of the MEPCs responding to each release of quantum of ACh both in time during evolution of an EPC and in space for a certain area of the postsynaptic membrane. Therefore, it is expected that localization of the release area of ACh related to the structure of the synaptic vesicles also has significant effects on generation of the EPC. The similar analysis to the case of the MEPC is performed to examine the effects of the localization of the ACh release area on the

behavior of $C(t)$ responding to many quantal releases of ACh with variation in the values of the radius ($25\text{nm} \leq d \leq 500\text{nm}$).

Though three dimensions in space are required to represent the summation of MEPC in time and in space, the compartment model with the parameters of $L = 500\text{nm}$, $N_r = 32$, $N_t = 1$, $F_w = 0$ (foldless), and $a = \infty$ (instantaneous release mechanism of ACh) is employed with the assumption of simultaneous release of all quanta of ACh. Supposing that a number of quantal release of ACh synchronously occur at the respective grid points distributed uniformly on the presynaptic membrane, the ACh molecules movable in the space corresponding to the grid point do not diffuse beyond the edge of the space because the exactly same processes are proceeding in the neighboring spaces. Therefore, it could be assumed that the EPC resulted from the spatial summation of the MEPC is linearly correlated to the $C(t)$ generated under the closed boundary conditions as follows:

$$\begin{aligned} \frac{\partial A(x,r,t)}{\partial x} &= 0 \quad \text{at} \quad x=0 \quad \text{and} \quad x=w\ ; \\ \frac{\partial A(x,r,t)}{\partial r} &= 0 \quad \text{at} \quad r=0 \quad \text{and} \quad r=L \end{aligned} \tag{5.1}$$

so that ACh cannot leak out from the disc.

The effects of the radius of the release area in the range of $25 \leq d \leq 500$ (nm) on the characteristic parameters of $C(t)$ are displayed in Fig. 5.3. The change in the size of the ACh release area has significant effects on $C(t)$. The behavior of $C(t)$ with variation in the radius of ACh release area is similar to the case of the MEPC, except for the corresponding values at the radius of 500nm. Every characteristic values are the same regardless of the values of $D_r$ at the radius of 500nm which corresponds to the homogeneous release of ACh.

The ratios of every characteristic values of $C(t)$ with the localized release area of ACh ($d = 50\text{nm}$) to those by the homogeneous release of ACh are given in Table 5.3, indicating that the localization of the ACh release has significant effect on the amplitude of $C(t)$, while the other parameters ($t_m$ and $\tau$) are less affected, equivalently to the case of generation of the MEPC. The difference in the effect between the amplitude and the other two parameters is obvious in the range of $D_r$ between $(1.0 \sim 2.0) \times 10^{-6}\text{cm}^2\text{sec}^{-1}$ in which the amplitude $C_{max}$ produced by the localized release area is about 2-fold of that by the homogeneous release of

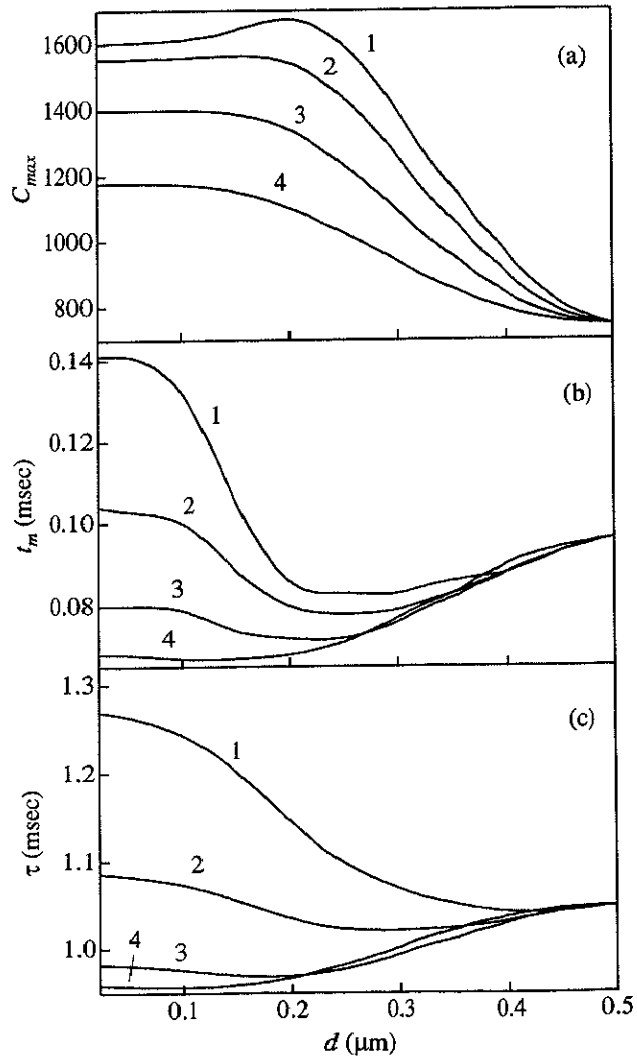


**Fig.5.3.** Effects of the radius $d$ of the ACh release area on the response of the total number of the open channel form of AChR in the case of generation of the EPC. Effects on: (a) the amplitude, (b) the growth time, (c) the decay constant. The number on a curve corresponds to the value of $D_r$ (in $10^{-6}\text{cm}^2\text{sec}^{-1}$): 1: 0.5, 2: 1.0, 3: 2.0, and 4: 4.0. The unit of $C(t)$ on the ordinate is the number of the open channel form of AChR.

**Table 5.3** Variation of the characteristic parameters of the EPC with diffusion coefficients

| $D_r$ ($\times 10^{-6}$cm$^2$sec$^{-1}$) | $C_{max}$(relative) | $t_m$ (relative) | $\tau$ (relative) |
|---|---|---|---|
| 0.50 | 2.15 | 1.47 | 1.21 |
| 1.00 | 2.08 | 1.07 | 1.03 |
| 2.00 | 1.87 | 0.83 | 0.93 |
| 4.00 | 1.58 | 0.71 | 0.91 |

"relative": ratios of the value with the release area of 50nm radius to that by homogeneous release of ACh

ACh, while the values of the other parameters vary around 15%.

In conclusion, the similar effects of the quantal release mechanism are also observed in the case of generation of the EPC. It is suggested that the localization of the release area of ACh has again significant effects on generation of the EPC, especially on the amplitude which gets higher by a factor about 2 compared with that by the homogeneous release of ACh.

## 5.3 Concluding remarks

The two-dimensional compartment model is applied to the analysis of the effects of the junctional fold on generation of the MEPC [21]. The simulation analysis reveals that the junctional fold causes the substantial effects, which might be relevant to the phenomenon of the notable spread of the growth time $t_m$ [30]. It is also found that the width of the junctional fold has more distinctive effects than the depth, implying that the radial diffusion process of ACh has more distinctive effects on the MEPC than the transverse process. This is similarly observed in the analysis for the effects of the anisotropic diffusion process as described in Section 4.1 [23]. The Friboulet's model [7], in which the depth of the junctional fold is represented with the thickness of the disc ($w$ in this study), is not satisfactory because the diffusion process in the radial direction is simplified as a simple efflux of ACh due to concentration gradient.

In the two-dimensional compartment model the amplitude of the MEPC may be maximized at an optimal value of the width of the junctional fold, suggesting that the folds enlarge the reacting area of the postsynaptic membrane. The Monte Calro procedure by the three-dimensional model with a junctional fold in actually folded shape yields the opposite results to this study that the amplitude $C_{max}$ and the growth time $t_m$ decrease but the decay constant $\tau$ does not change with addition of more junctional folds [2]. Possibly, the folded shape of the junctional fold, instead of cylinder for the model in this study, may cause the difference. The actual shape of the junctional folds in three-dimensional space should be taken into account for modeling and analysis. Extension of the two-dimensional model to a three-dimensional model is required for full elucidation of the correlations between the functions and the structures of the chemical transmission process.

The compartment model is further applied to examine the effects of the quantal release mechanism of ACh. The simulation analysis demonstrates that the localization of the ACh release due to the structure of the synaptic vesicles has significant effect on the amplitudes of MEPC and EPC. The amplitude of the EPC generated by the localized release of ACh is about double of that by the homogeneous release of ACh. The effect of the localized release might be due to the interaction mechanism between ACh and AChR since the dimeric AChR

requires a certain concentration of ACh to open the ion channel. It is considered that the interaction mechanism also works for the rapid decline of MEPC, so that the cooperation of the dimeric structure of AChR and the localized release of ACh due to the structure of the synaptic vesicle is intrinsic for the optimal shape of the MEPC and EPC. This consideration could be examined on the comparison of the dynamic behavior of RD system with imaginal monomeric AChR.

The quantal release mechanism of ACh is represented with the radius of the pore ($\rho$) for the release rate of ACh into the cleft in Section 4.2, and with the radius of the release area ($d$) for the localization of the release area of ACh in the cleft in this section. Though it is natural to assume that the radius of the pore is equal to the radius of the release area, the two parameters are analyzed independently because of the difficulty in the construction of the compartment model as mentioned in Section 3.1. The integration of these parameters is required for modeling of more realistic release mechanism.

# Chapter 6

# Conclusion

A compartment model representing the chemical transmission process of ACh at the neuromuscular junction for generation of the MEPC is constructed as an RD system in a two-dimensional space of axis-symmetrical disc of the synaptic cleft. The model is defined as the standard for the critical radius of 500nm and the respective compartment numbers of 3 and 10 on the transverse and radial coordinates. Besides the transverse and radial diffusion processes, the model includes the release mechanism of ACh as the release rate and the release area of ACh, and the junctional fold as a concentric cylinder with its top surface attached to the bottom of the disc to open a hole to the synaptic cleft at the postsynaptic membrane. The model might be regarded as the two-dimensional extension of the similar models proposed previously [7, 26, 32], which essentially behave as one-dimensional compartment models because the diffusion process in either of two directions is simplified.

This two-dimensional compartment model is effectively applied to analysis of the functional and structural correlations in the transmission process, especially, quantitative characterization of the RD system of ACh with respect to specific parameters, leading to estimation of unknown values of the parameters and elucidation of significance of the specific structures and functions associated with the neuromuscular junction. The parameters of diffusion coefficients of ACh in the synaptic cleft and of the ACh release mechanisms are characterized quantitatively by the simulation with the model. Another aspect of application of the model is concerned with the specific structures of the neuromuscular junction such as the junctional folds and the synaptic vesicles.

The simulation analysis for characterization of the diffusion coefficients of ACh demon-

strates that the diffusion coefficient for isotropic diffusion (i.e., $D_t = D_r$) in the disc is evaluated to be $1.0 \times 10^{-6}\text{cm}^2\text{sec}^{-1}$, with which the model reproduces the behavior of the MEPC from the empirical analysis with respect to the characteristic parameters. It further follows from individual variation in $D_t$ and $D_r$ that the radial diffusion has more distinctive effects than the transverse diffusion, that is, in the RD system with anisotropic diffusion, increase in $D_r$ significantly reduces all of $C_{max}$, $t_m$ and $\tau$. Moreover, the effects of $D_t$ are still less discernible at smaller $D_r$.

The neurotransmitter release mechanism is also analyzed with the model to reveal that the natural diffusion through a pore of a fixed radius of 1.0nm, which is evaluated as the initial radius [12, 29, 30], is not sufficient for reproduction of the empirical data and that some mechanism additional to the natural diffusion is required for the model to represent appropriately the generation of MEPC. The mechanism of the expanding pore thus is examined to infer that it could reproduce the empirical MEPC with the expanding rate more than 10nm/msec and with the diffusion coefficient of 0.5 or 1.0 ($\times 10^{-6}\text{cm}^2\text{sec}^{-1}$). The acceleration mechanism for the release of ACh is found to work satisfactorily with the acceleration rate 10 times of the natural diffusion and with the diffusion coefficient of 0.5 or 1.0 ($\times 10^{-6}$ $\text{cm}^2\text{sec}^{-1}$).

The simulation analysis for the function of the junctional fold discloses that the junctional fold causes the substantial effects on the generation of MEPC and that the width of the junctional fold has more distinctive effects than the depth, implying again that the radial diffusion process of ACh has more distinctive effects on the MEPC than the transverse process. It is also found that the amplitude of the MEPC may be maximized at an optimal value of the width of the junctional fold, suggesting that the folds enlarge the reacting area of the postsynaptic membrane.

For further application, the simulation analysis is performed with the model to clarify the biochemical significance of the quantal release mechanism of ACh with respect to generation of the MEPC. It is revealed that the mechanism raises the amplitude of MEPC significantly. The evaluation of the size of the release area of ACh is furthermore attempted with regard to the EPC responding to arrival of the action potential at the nerve terminal. The same

effect of the quantal release mechanism is again assured in the case of EPC. The localized release of ACh makes the amplitude of EPC higher by a factor about 2 compared with that in the homogeneous release of ACh, implying that the quantal release mechanism works as an amplifier of the EPC with the fixed amount of ACh available.

The two-dimensional compartment model constructed and applied in this study is thus valuable for analysis of the functional and structural correlations in the chemical transmission process. Further application and extention of the model would contribute more to elucidation of the mechanisms in the synaptic signal transmission.

The author is grateful to Prof. Naoto Sakamoto of the University of Tsukuba for guidance of the research and completion of the dissertation.

# Bibliography


[1] L. Anglister, J. R. Stiles, and M. M. Salpeter. Acetylcholinesterase density and turnover number at frog neuromuscular junctions, with modeling of their role in synaptic function. *Neuron*, 12:783–794, 1994.

[2] J. Bartol, T. M., B. R. Land, E. E. Salpeter, and M. M. Salpeter. Monte Carlo simulation of miniature endplate current generation in the vertebrate neuromuscular junction. *Biophys. J.*, 59:1290–1307, 1991.

[3] M. Berzins. Global error estimation in the method of lines for parabolic equations. *SIAM J. Sci. Stat. Comput.*, 9:687–702, 1988.

[4] M. Bieterman and I. Babuska. An adaptive method of lines with error control for parabolic equations of the reaction-diffusion type. *J. Comput. Phys.*, 63:33–66, 1986.

[5] R. Birks, H. E. Huxley, and B. Katz. The fine structure of the neuromuscular junction of the frog. *J. Physiol.*, 150:134–144, 1960.

[6] M. Brzin, J. Sketelj, Z. Grubic, and T. Kiauta. Cholinesterases of neuromuscular junction. *Neurochem. Int.*, 2:149–159, 1980.

[7] A. Friboulet and D. Thomas. Reaction-diffusion coupling in a structured system: application to the quantitative simulation of endplate currents. *J. theor. Biol.*, 160:441–455, 1993.

[8] G. W. Gear. *Numerical Initial Value Problems in Ordinary Differential Equations.* Prentice-Hall, Englewood Cliffs, 1971.

[9] L. Graney and A. A. Richardson. The numerical solution of non-linear partial differential equations by the method of lines. *J. Comput. Appl. Math.*, 7:229–236, 1981.

[10] K. Hayashi and N. Sakamoto. *Dynamic Analysis of Enzyme Systems.* JSSP/Springer-Verlag, Tokyo/Berlin, 1986.

[11] B. Katz and R. Miledi. The binding of acetylcholine to receptors and its removal from the synaptic cleft. *J. Physiol.*, 231:549–574, 1973.

[12] R. Khanin, H. Parnas, and L. Segel. Diffusion cannot govern the discharge of neurotransmitter in fast synapses. *Biophys. J.*, 67:966–972, 1994.

[13] R. E. Krnjevic and J. F. Mitchell. Diffusion of acetylcholine in agar gels and in the isolated rat diaphragm. *J. Physiol.*, 153:562–577, 1960.

[14] B. R. Land, W. V. Harris, E. E. Salpeter, and M. M. Salpeter. Diffusion and binding constants for acetylcholine derived from the falling phase of miniature endplate currents. *Proc. Natl. Acad. Sci. USA*, 81:1594–1598, 1984.

[15] B. R. Land, E. E. Salpeter, and M. M. Salpeter. Kinetic parameters for acetylcholine interaction in intact neuromuscular junction. *Proc. Natl. Acad. Sci. USA*, 78:7200–7204, 1981.

[16] MathWorks. *Simulink User's Guide.* The MathWorks, Inc., Natick, MA, 1992.

[17] G. G. Matthews. *Cellular Physiology of Nerve and Muscle*, Blackwell Scientific Publications, Palo Alto, 1986.

[18] G. G. Matthews. Neurotransmitter release. *Annu. Rev. Neurosci.*, 19:219–233, 1996.

[19] U. Matthews-Bellinger and M. M. Salpeter. Distribution of acetylcholine receptors at frog neuromuscular junctions with a discussion of some physiological implications. *J. Physiol.*, 279:179–213, 1978.

[20] R. Miledi, P. C. Molenaar, and R. L. Polak. Acetylcholinesterase activity in intact and homogenized skeletal muscle of the frog. *J. Physiol.*, 349:663–686, 1984.

[21] T. Naka. Simulation analysis of the effects of the junctional folds on spontaneous generation of the miniature endplate current at the neuromuscular junction. *Proceedings of 2nd Mathmod Vienna*, pp. 943–948, Technical University Vienna, Austria, 1997.

[22] T. Naka and N. Sakamoto. Kinetics of membrane-bound enzymes: Validity of quasi-steady-state approximation for a Michaelis-Menten-type reaction. *J. Membrane Sci.*, 74:159–170, 1992.

[23] T. Naka, K. Shiba, and N. Sakamoto. A two-dimensional compartment model for the reaction-diffusion system of acetylcholine in the synaptic cleft at the neuromuscular junction. *BioSystems*, 41:17–27, 1997.

[24] L. D. Partridge and L. D. Partridge. Chemical effectors. In *The Nervous System: Its Function and Its Interaction with the World*, pp. 297–326, MIT Press, Cambridge, 1992.

[25] T. L. Rosenberry. Acetylcholinesterase. *Adv. Enzymol.*, 43:103–218, 1975.

[26] T. L. Rosenberry. Quantitative simulation of endplate currents at neuromuscular junctions based on the reaction of acetylcholine with acetylcholine receptor and acetylcholinesterase. *Biophys. J.*, 26:263–290, 1979.

[27] W. E. Schiesser. *The Numerical Method of Lines: Integration of Partial Differential Equations.* Academic Press, San Diego, 1991.

[28] A. E. Spruce, L. J. Breckenridge, A. K. Lee, and W. Almers. Properties of the fusion pore that forms during exocytosis of a mast cell secretory vesicle. *Neuron*, 4:643–654, 1990.

[29] J. R. Stiles, D. Van Helden, J. Bartol, T. M., E. E. Salpeter, and M. M. Salpeter. Miniature endplate current rise time $< 100\mu s$ from improved dual recordings can be modeled with passive acetylcholine diffusion from a synaptic vesicle. *Proc. Natl. Acad. Sci. USA*, 93:5747–5752, 1996.

[30] W. Van der Kloot. The rise times of miniature endplate currents suggest that acetylcholine may be released over a period of time. *Biophys. J.*, 69:148–154, 1995.

[31] W. Van der Kloot and J. Molgo. Quantal acetylcholine release at the vertebrate neuromuscular junction. *Physiol. Rev.*, 74:899–991, 1994.

[32] U. C. Wathey, M. M. Nass, and H. A. Lester. Numerical reconstruction of the quantal event at nicotinic synapses. *Biophys. J.*, 27:145–164, 1979.

# Appendix

# S-functions of the differential equations

The RD system representing the dynamic behavior of ACh in the cleft is formulated as a set of partial differential equations, which is discretized on the space coordinates to lead to a set of ordinary differential equations as given in Section 3.1. The Gear method is then applied to the ordinary differential equations to yield the temporal variation in concentrations of the chemical species in the RD system. In this appendix the full representation of the derived ordinary differential equations is provided in the form of S-function, which is syntactically C language.

SIMULINK is employed for numerical integration of the ordinary differential equations derived from the RD system. SIMULINK, one of the extensions of MatLab [16], consists of a set of programs for simulating dynamic systems. The procedure of the simulation analysis as

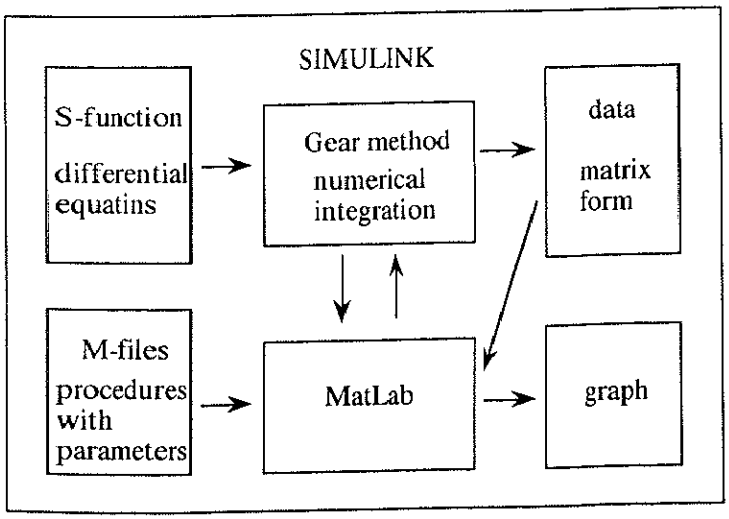


**Fig.A.1.** The procedure of the analysis using SIMULINK.

shown in Fig. A.1 begins with formulation of the set of ordinary differential equations as the S-function which is the executable form of SIMULINK. The kinetic and structural parameters of the RD system and the initial conditions are processed with the M-files in SIMULINK. Operation of the function of Gear, which is one of the numerical integration algorithm of SIMULINK, yields the time courses of the concentration in the respective chemical species in the RD system as the matrix forms of MatLab. Such data are easily visualized with the graphic feature of MatLab.

Two versions of the S-functions are formulated in this study. The version for the instantaneous release of ACh is applied for the analysis in Sections 4.1, 5.1, 5.2, and the corresponding analysis in Section 3.1. The other version for the ACh release mechanisms without the junctional fold is employed for the analysis in Section 4.2.

The executions of numerical integration are performed on the interactive interface of the MatLab or on scripts written as the form of M-files of MatLab. The procedures with the set of the parameters and the initial conditions for the respective analysis are shown as the form of M-files in the last section.

# 1. The model for the instantaneous release of ACh

The following S-function formulates the RD system with the open boundary conditions as expressed in Eqn.3.3. For the simulation of the EPC, one of the define-statements should be replaced with a define-statement corresponding to the closed boundary condition as expressed in Eqn.5.1 according to the comment in the program list.

```
/*************************************************************************
 *
 * The model of the RD system for the chemical transmission process
 *           at the neuromuscular junction with a juncional fold,
 *           assuming the instantaneous release of ACh.
 *
 *  Geometry
 *
 *
 *          <------------ r --------------+
 *                                        |<RVN>|
 *          |-----------RC<NRD>-----------|
 *    +     +-------------------------+ (Ach) +-------------------------+
 *    |     |/////////////////////////////|////////////////////////////////|
 * WX<NXD>  |/////////////////////////////|////////////////////////////////|
 *    |     |////////////////////////(AchE)////////////////////////////////|
 *    +   + @@@@@@@@@@@@@@@@@@@@@@@@@@@@@/////|/////@@@@@@@@@@@@@@@@@@@@@@@@@@@@
 *    |   |          (AchR)                 @/////|/////@
 *    |   |                                 @/////|/////@
 *    | <DEN>                               @/////|/////@
 *    |   |                                 @/////|/////@
 *    |   |                                 @/////|/////@
 *    |   +                                 @/////|/////@
 * DF<NFD>                                  |     |     |
 *    |                                     |     x     |
 *    |                                     |     |     |
 *    |                                     |     |     |
 *    |                                     |     |     |
 *    +                                     +-----|-----+
 *                                          |<RFN>|
 *                                                |
 *                                                Y
 *  Zoning
 *          +-----------------------------------+
 *          |                Zone1              |
 *          +---------------+---+---------------+
 *                          |   |
 *                          | Z |
 *                          | o |
 *                          | n |
 *                          | e |
 *                          | 2 |
 *                          |   |
 *                          +---+
 *
```

```
*  Differential equations
*
*       d[A]   /dt    = DR*( dd[A]/drr + 1/r*d[A]/dr ) + DX*dd[A]/dxx
*                     + KM1[AE] - K1[A][E]
*                     + Exist_Ach(x,r)*( KMR*( [AR] + 2[AAR] )
*                     - KR*A*( 2[R] + [AR] ) )
*
*       d[AE] /dt     = K1[A][E] - ( KM1 + K2 )[AE]
*       d[Eac]/dt     = K2[AE] - K3[Eac]
*       d[AR] /dt     = KR[A]*( 2[R] - [AR] ) + KMR*( 2[AAR] - [AR] )
*       d[AAR]/dt     = KR[A][AR] - 2KMR[AAR] + KC[O] - KO[AAR]
*       d[O]   /dt    = KO[AAR] - KC[O]
*
*  Consevation laws
*
*       ET   = [E] + [AE] + [Eac]
*       RT   = [R] + [AR] + [AAR] + [O]
*
*  Boundary conditions
*
*       dA(x,*)/dx = 0
*       dA(*,r)/dr = 0
*       A (*,RC)   = 0
*
*  Variables for chemical species
*
*       A(x,r)  A   Acetylcoline(Ach)
*       E(x,r)  E   Free acetylcolinesterase(AchE)
*       B(x,r)  AE  Ach-AchE Michaelis complex
*       F(x,r)  Eac Ach-AchE intermediate acetylated complex
*       R(r)    R   Acetylcoline recptor(AchR)
*       U(r)    AR  Ach-AchR closed channel assembly
*       V(r)    AAR Ach-Ach-AchR closed channel assembly
*       O(r)    O   Ach-Ach-AchR open channel assembly
*
*  Parameters (in mM-msec-microm system)
*
*       Rate constants for reactions
*           K1  200 A + E -> AE
*           KM1 1   A + E <- AE
*           K2  110 AE    -> Eac
*           K3  20  Eac   -> E + acetate + H2
*           KR  30  A + R -> AR
*           KMR 10  A + R <- AR
*           KO  20  AAR   -> O
*           KC  5   AAR   <- O
*
*       Diffusion coefficients for Ach
*           DX  0.1 Crossing
*           DR  0.1 Radial
*
*       Structure of synapse
*           WX  0.05    Width of the cleft          ( != 0 )
*           DF  0.5     Depth of the fold           ( != 0 )
*           RC  0.5     Radius of the critical disc ( != 0 )
*           ST  9000    Surface area of membrane
*
```

```
*      Substrates
*          NA  1e4 Total Ach released per MEPC
*          NE  2e7 Total esterase in the cleft
*          CR  2e4 Surface density of receptors
*
*      Number of discritizatins
*          NXD 1   Crossing in the cleft
*          NFD 10  Crossing in the fold
*          NRD 10  Radial
*          RVN 1   Radius of the synaptic vesicles
*          RFN 1   Radius of the synaptic folds
*          DEN 5   Depth of the folds with AchR & AchE
*
*      Etc
*          PI  3.1415  Pai
*          AVM 6.022e5 Avogadro's number in this units
*              = 6.022e23 / ( 1e15 * 1e3 )
*                  1e15    1 liter = CL mivro-m^3
*                  1e3 1 M     = CM mM
*
*  Drived constants
*
*      VT   ST*WX          Volume of the cleft
*      SC1                 Area of membrane with AchR in zone1
*      RF   RC*RFN/NRD     Radius of the fold
*      DE   DF*DEN/NFD     Depth of the fold with AchR & AchE
*      SC2  2*PI*RF*DE     Area of membrane with AchR in zone2
*      RV   RC*RVN/NRD     Radius of the synaptic vesicle
*      SV   PI*RV^2        Area of the Ach influxing disc
*      VV   SV*WX/NXD      Volume of the release area of ACh
*      VC1  SC1*WX/NXD     Volume of a compartment with AchR in zone1
*      VC2  PI*RF^2*(2*RFN-1)*DE/RFN^2                       in zone2
*
*      RT1  CR*SC1/(VC1*AVM)= CR*NXD/(WX*AVM)       AchR conc.in zone1
*      RT2  CR*SC2/(VC2*AVM)= CR*RFN*NRD/((RFN-1/2)*RC*AVM)   in zone2
*      ET   NE/(VT*AVM)     = NE/(ST*WX*AVM)        AchE conc.
*      AT   NA/(VV*AVM)     = NA*NXD/(SV*WX*AVM)    Ach conc. per MEPC
*
**************************************************************************/
#include    "matrix.h"

#define     AVM     6.022e5
#define     PI      3.1415

#define     NSTATES     2380            /* NRD*NXD*4 + (NRD-RFN)*4          */
                                        /* + RFN*NFD + RFN*DEN*3 + DEN*4    */
#define     NCOEFFS     1
#define     NINPUTS     0
#define     NOUTPUTS    1               /* Number of open channels          */

static      Matrix      *Coeffs[NCOEFFS];
#define     K1          mxGetPr(Coeffs[0])[0]
#define     KM1         mxGetPr(Coeffs[0])[1]
#define     K2          mxGetPr(Coeffs[0])[2]
#define     K3          mxGetPr(Coeffs[0])[3]
#define     KR          mxGetPr(Coeffs[0])[4]
#define     KMR         mxGetPr(Coeffs[0])[5]
```

```
#define     KO          mxGetPr(Coeffs[0])[6]
#define     KC          mxGetPr(Coeffs[0])[7]
#define     DX          mxGetPr(Coeffs[0])[8]
#define     DR          mxGetPr(Coeffs[0])[9]
#define     WX          mxGetPr(Coeffs[0])[10]
#define     DF          mxGetPr(Coeffs[0])[11]
#define     RC          mxGetPr(Coeffs[0])[12]
#define     ST          mxGetPr(Coeffs[0])[13]
#define     NA          mxGetPr(Coeffs[0])[14]
#define     NE          mxGetPr(Coeffs[0])[15]
#define     CR          mxGetPr(Coeffs[0])[16]
#define     RNXD        mxGetPr(Coeffs[0])[17]
#define     RNFD        mxGetPr(Coeffs[0])[18]
#define     RNRD        mxGetPr(Coeffs[0])[19]
#define     RRVN        mxGetPr(Coeffs[0])[20]
#define     RRFN        mxGetPr(Coeffs[0])[21]
#define     RDEN        mxGetPr(Coeffs[0])[22]

#define     I1(X,R)     (NRD*(X)+(R))
#define     I2(X,R)     (NFD*(R)+(X))
#define     I3(X,R)     (DEN*(R)+(X))

#define     IA1(X,R)    (I1(X,R))
#define     IB1(X,R)    (OF11+I1(X,R))
#define     IF1(X,R)    (OF12+I1(X,R))
#define     IE1(X,R)    (OF13+I1(X,R))
#define     IU1(R)      (OF14+(R))
#define     IV1(R)      (OF15+(R))
#define     IO1(R)      (OF16+(R))
#define     IR1(R)      (OF17+(R))

#define     IA2(X,R)    (OF21+I2(X,R))
#define     IB2(X,R)    (OF22+I3(X,R))
#define     IF2(X,R)    (OF23+I3(X,R))
#define     IE2(X,R)    (OF24+I3(X,R))
#define     IU2(X)      (OF25+(X))
#define     IV2(X)      (OF26+(X))
#define     IO2(X)      (OF27+(X))
#define     IR2(X)      (OF28+(X))

#define     A10(X,R)    xO[IA1(X,R)]
#define     B10(X,R)    xO[IB1(X,R)]
#define     F10(X,R)    xO[IF1(X,R)]
#define     E10(X,R)    xO[IE1(X,R)]
#define     U10(R)      xO[IU1(R)]
#define     V10(R)      xO[IV1(R)]
#define     O10(R)      xO[IO1(R)]
#define     R10(R)      xO[IR1(R)]

#define     A20(X,R)    xO[IA2(X,R)]
#define     B20(X,R)    xO[IB2(X,R)]
#define     F20(X,R)    xO[IF2(X,R)]
#define     E20(X,R)    xO[IE2(X,R)]
#define     U20(X)      xO[IU2(X)]
#define     V20(X)      xO[IV2(X)]
#define     O20(X)      xO[IO2(X)]
#define     R20(X)      xO[IR2(X)]
```

```
#define     A1P(X,R)    ((R)<RFN?x[IA2(0,R)]:x[IA1(NXD-1,R)])
#define     A1Q(X,R)    ((X)<0?x[IA1(0,R)]:((X)<NXD?x[IA1(X,R)]:A1P(X,R)))

/* For the simulation of EPC, the following define statement should be     */
/*                                                          replaced with: */
/* #define  A1(X,R)     ((R)>=NRD?A1Q(X,(NRD-1):((R)<0?A1Q(X,0):A1Q(X,R))) */

#define     A1(X,R)     ((R)>=NRD?0:((R)<0?A1Q(X,0):A1Q(X,R)))
#define     B1(X,R)     x[IB1(X,R)]
#define     F1(X,R)     x[IF1(X,R)]
#define     E1(X,R)     x[IE1(X,R)]
#define     U1(R)       x[IU1(R)]
#define     V1(R)       x[IV1(R)]
#define     O1(R)       x[IO1(R)]
#define     R1(R)       x[IR1(R)]

#define     A2P(X,R)    ((X)<NFD?x[IA2(X,R)]:x[IA2(NFD-1,R)])
#define     A2Q(X,R)    ((X)<0?x[IA1(NXD-1,R)]:A2P(X,R))

#define     A2(X,R)     ((R)>=RFN?A2Q(X,RFN-1):((R)<0?A2Q(X,0):A2Q(X,R)))
#define     B2(X,R)     x[IB2(X,R)]
#define     F2(X,R)     x[IF2(X,R)]
#define     E2(X,R)     x[IE2(X,R)]
#define     U2(X)       x[IU2(X)]
#define     V2(X)       x[IV2(X)]
#define     O2(X)       x[IO2(X)]
#define     R2(X)       x[IR2(X)]

#define     dA1(X,R)    dx[IA1(X,R)]
#define     dB1(X,R)    dx[IB1(X,R)]
#define     dF1(X,R)    dx[IF1(X,R)]
#define     dE1(X,R)    dx[IE1(X,R)]
#define     dU1(R)      dx[IU1(R)]
#define     dV1(R)      dx[IV1(R)]
#define     dO1(R)      dx[IO1(R)]
#define     dR1(R)      dx[IR1(R)]

#define     dA2(X,R)    dx[IA2(X,R)]
#define     dB2(X,R)    dx[IB2(X,R)]
#define     dF2(X,R)    dx[IF2(X,R)]
#define     dE2(X,R)    dx[IE2(X,R)]
#define     dU2(X)      dx[IU2(X)]
#define     dV2(X)      dx[IV2(X)]
#define     dO2(X)      dx[IO2(X)]
#define     dR2(X)      dx[IR2(X)]

static  int NXD;
static  int NFD;
static  int NRD;
static  int RVN;
static  int RFN;
static  int DEN;

static  int TNC1;       /* Total number of compartments in zone 1 */
static  int TNC2;       /* Total number of compartments in zone 2 */
static  int TNR1;       /* Total number of compartments for AchR in zone 1 */
```

```
static  int TNE2;       /* Total number of compartments for AchE in zone 2 */
static  int OF11, OF12, OF13, OF14, OF15, OF16, OF17;
static  int OF21, OF22, OF23, OF24, OF25, OF26, OF27, OF28;

static  double  U1X;                            /* Delta x in zone1 */
static  double  U2X;                            /* Delta x in zone2 */
static  double  UR;                             /* Delta r */
static  double  D1X2;                           /* DX/(U1X*U1X) */
static  double  D2X2;                           /* DX/(U2X*U2X) */
static  double  DR2;                            /* DR/(UR*UR) */
static  double  OCE1;                           /* for outputs in zone 1 */
static  double  OCE2;                           /* for outputs in zone 2 */

void    init_conditions(x0)
double  *x0;
    {
    double  RT1 = CR*RNXD/(WX*AVM);
    double  RT2 = CR*RRFN*RNRD/((RRFN-1.0/2.0)*RC*AVM);
    double  ET  = NE/(ST*WX*AVM);
    double  RV  = RC*RRVN/RNRD;
    double  AT  = NA*RNXD/(PI*RV*RV*WX*AVM);
    int i,j;

    NXD  = RNXD + 0.5;
    NFD  = RNFD + 0.5;
    NRD  = RNRD + 0.5;
    RVN  = RRVN + 0.5;
    RFN  = RRFN + 0.5;
    DEN  = RDEN + 0.5;

    TNC1 = NRD*NXD;     /* Total number of compartments in zone 1 */
    TNC2 = NFD*RFN;     /* Total number of compartments in zone 2 */
    TNR1 = NRD - RFN;   /* Total number of compartments for AchR in zone 1 */
    TNE2 = DEN*RFN;     /* Total number of compartments for AchE in zone 2 */

    OF11 = TNC1;        /* Offsets for references to variables */
    OF12 = OF11 + TNC1;
    OF13 = OF12 + TNC1;
    OF14 = OF13 + TNC1;
    OF15 = OF14 + TNR1;
    OF16 = OF15 + TNR1;
    OF17 = OF16 + TNR1;
    OF21 = OF17 + TNR1;
    OF22 = OF21 + TNC2;
    OF23 = OF22 + TNE2;
    OF24 = OF23 + TNE2;
    OF25 = OF24 + TNE2;
    OF26 = OF25 + DEN;
    OF27 = OF26 + DEN;
    OF28 = OF27 + DEN;

    U1X  = WX/NXD;
    U2X  = DF/NFD;
    UR   = RC/NRD;
    D1X2 = DX/(U1X*U1X);
    D2X2 = DX/(U2X*U2X);
    DR2  = DR/(UR*UR);
```

```
    OCE1 = PI*UR*UR*U1X*AVM;                    /* for outputs in zone 1 */
    OCE2 = PI*UR*UR*(2*RFN-1)*U2X*AVM;          /* for outputs in zone 2 */

    for( i = 0; i < NXD; i++ )                  /* for zone 1 */
        for( j = 0; j < NRD; j++ )
            {
            A10(i,j) = B10(i,j) = F10(i,j) = 0.0;
            E10(i,j) = ET;
            }
    for( j = 0; j < TNR1; j++ )
        {
        U10(j) = V10(j) = O10(j) = 0.0;
        R10(j) = RT1;
        }
    for( j = 0; j < RVN; j++ )
        A10(0,j) = AT;
    for( i = 0; i < DEN; i++ )                  /* for zone 2 */
        {
        for( j = 0; j < RFN; j++ )
            {
            A20(i,j) = B20(i,j) = F20(i,j) = 0.0;
            E20(i,j) = ET;
            }
        U20(i) = V20(i) = O20(i) = 0.0;
        R20(i) = RT2;
        }
    for( i = DEN; i < NFD; i++ )
        for( j = 0; j < RFN; j++ )
            A20(i,j) = 0.0;
    }

void    derivatives(t,x,u,dx)
    double  t,*x,*u;
    double  *dx;
    {
    double  f1, f2, f3, f4, f5, f6;
    int i,j;

    for( i = 0; i < NXD; i++ )                  /* for zone 1 */
        for( j = 0; j < NRD; j++ )
            {
            f1  = - K1*E1(i,j)*A1(i,j) + KM1*B1(i,j);
            f2  = K2*B1(i,j);
            f3  = K3*F1(i,j);
            dA1(i,j) = f1 + D1X2*( A1(i-1,j) - 2*A1(i,j) + A1(i+1,j) )
                + DR2*( A1(i,j-1) - 2*A1(i,j) + A1(i,j+1)
                + ( A1(i,j+1) - A1(i,j-1) )/( 2*( j + 0.5 ) ) );
            dB1(i,j) = - f1 - f2;
            dF1(i,j) = f2 - f3;
            dE1(i,j) = f1 + f3;
            }
    for( j = 0; j < TNR1; j++ )
        {
        f4  = - 2*KR*A1(NXD-1,j+RFN)*R1(j) + KMR*U1(j);
        f5  = - KR*A1(NXD-1,j+RFN)*U1(j) + 2*KMR*V1(j);
        f6  = KO*V1(j) - KC*O1(j);
        dA1(NXD-1,j+RFN) += f4 + f5;
```

```
        dU1(j)  = - f4 + f5;
        dV1(j)  = - f5 - f6;
        dO1(j)  = f6;
        dR1(j)  = f4;
        }

    for( i = 0; i < DEN; i++ )                  /* for zone 2 */
        {
        for( j = 0; j < RFN; j++ )
            {
            f1  = - K1*E2(i,j)*A2(i,j) + KM1*B2(i,j);
            f2  = K2*B2(i,j);
            f3  = K3*F2(i,j);
            dA2(i,j) = f1 + D2X2*( A2(i-1,j) - 2*A2(i,j) + A2(i+1,j) )
                + DR2*( A2(i,j-1) - 2*A2(i,j) + A2(i,j+1)
                + ( A2(i,j+1) - A2(i,j-1) )/( 2*( j + 0.5 ) ) );
            dB2(i,j) = - f1 - f2;
            dF2(i,j) = f2 - f3;
            dE2(i,j) = f1 + f3;
            }
        if( RFN > 0 )
            {
            f4  = - 2*KR*A2(i,RFN-1)*R2(i) + KMR*U2(i);
            f5  = - KR*A2(i,RFN-1)*U2(i) + 2*KMR*V2(i);
            f6  = KO*V2(i) - KC*O2(i);
            dA2(i,RFN-1) += f4 + f5;
            dU2(i)  = - f4 + f5;
            dV2(i)  = - f5 - f6;
            dO2(i)  = f6;
            dR2(i)  = f4;
            }
        }
    for( i = DEN; i < NFD; i++ )
        for( j = 0; j < RFN; j++ )
            dA2(i,j) = D2X2*( A2(i-1,j) - 2*A2(i,j) + A2(i+1,j) )
                + DR2*( A2(i,j-1) - 2*A2(i,j) + A2(i,j+1)
                + ( A2(i,j+1) - A2(i,j-1) )/( 2*( j + 0.5 ) ) );
    }

double  outputs(t,x,u,y)
    double  t,*x,*u;
    double  *y;
    {
    int i, j;
    double  osum;

    for( j = 0, osum = 0.0; j < TNR1; j++ )
        osum += ( 2*( j + RFN ) + 1 )*O1(j);
    y[0] = osum*OCE1;
    if( RFN > 0 )
        {
        for( i = 0, osum = 0.0; i < DEN; i++ ) osum += O2(i);
        y[0] += osum*OCE2;
        }
    }

#include        "simulink.h"
```

## 2. The model for the release mechanism of ACh

The following S-function formulates the RD system with the mechanisms for ACh release from the synaptic vesicle without the junctional fold.

```
/*********************************************************************
 *
 * The model of the RD syatem for the chemical transmission process
 *           at the neuromuscular junction
 *           with the release mechanisms of ACh.
 *
 *  Differential equations
 *
 *      d[A]  /dt   = DA*( dd[A]/dxx + dd[A]/drr + 1/r*d[A]/dr )
 *                  + KM1[AE] - K1[A][E]
 *                  + dlt( x - WX )*( KMR*( [AR] + 2[AAR] )
 *                                  - KR*A*( 2[R] + [AR] ) )
 *                  - dlt( x, r )*DSS*VV/VS*( [A] - [AS] )
 *
 *      d[AS] /dt   = DSS*( [A] - [AS] )
 *      d[AE] /dt   = K1[A][E] - ( KM1 + K2 )[AE]
 *      d[Eac]/dt   = K2[AE] - K3[Eac]
 *      d[AR] /dt   = KR[A]*( 2[R] - [AR] ) + KMR*( 2[AAR] - [AR] )
 *      d[AAR]/dt   = KR[A][AR] - 2KMR[AAR] + KC[O] - KO[AAR]
 *      d[O]  /dt   = KO[AAR] - KC[O]
 *
 *  Conservation laws
 *
 *      Et  = [E] + [Ae] + [Eac]
 *      RT  = [R] + [AR] + [AAR] + [O]
 *
 *  Boundary conditions
 *
 *      dA(0,*) /dx = 0
 *      dA(WX,*)/dx = 0
 *      dA(*,0) /dr = 0
 *      A (*,RC)    = 0
 *
 *  Equation for the release mechanisms
 *
 *      VC*A(0,0)   = -VV*S  ->
 *      dA(0,0)     = -VV/VS*dS
 *                  = -VV/VS*DSS*( A - S )
 *                  = -VV/VS*DS*PI*RP^2/(VV*LP)*( A - S )
 *                  = -DS*PI*RP^2/(VS*LP)*( A - S )
 *                  = -DS*PI*RP^2/(PI*UR^2*UX*LP)*( A - S )
 *                  = -DS*RP^2/(UR^2*UX*LP)*( A - S )
 *      S(0) = NA/(VV*AVM)
 *           = NA/(4/3*PI*RV^3*AVM)
 *
 *  Variables for chemical species
 *
 *      A(x,r)  A   Acetylcoline(Ach)
 *      S       AS  Ach in vesicle
 *      E(x,r)  E   Free acetylcolinesterase(AchE)
```

```
*      B(x,r)  AE  Ach-AchE Michaelis complex
*      F(x,r)  Eac Ach-AchE intermediate acetylated complex
*      R(r)    R   Free Acetylcoline recptor(AchR)
*      U(r)    AR  Ach-AchR closed channel assembly
*      V(r)    AAR Ach-Ach-AchR closed channel assembly
*      O(r)    O   Ach-Ach-AchR open channel assembly
*
*  Parameters (in mM/m-sec/micro-m system)
*
*      Rate constants for reactions
*          K1  200 A + E -> AE
*          KM1 1   A + E <- AE
*          K2  110 AE    -> Eac
*          K3  20  Eac   -> E + acetate + H2
*          KR  30  A + R -> AR
*          KMR 10  A + R <- AR
*          KO  20  AAR   -> O
*          KC  5   AAR   <- O
*
*      Diffusion coefficients for Ach
*          DA  0.1 in the cleft
*          DS  0.1 in the pore between the vesicle and the cleft
*
*      Structure of synapse
*          WX  0.05    Width of the cleft
*          RC  0.5     Radius of the critical disc
*          RV  1.85e-2 Radius of the vesicle
*          RP  1.00e-3 Initial radius of the pore
*          ER  2.50e-2 Expanding rate of the pore
*          FR  1.0     Factor of the outflow from the vasicle
*          LP  1.00e-2 Length of the pore
*          VC  450     Volume of the cleft
*
*      Substrates
*          NA  1e4 Total Ach released per MEPC
*          NE  2e7 Total esterase in the cleft
*          CR  2e4 Surface density of receptors
*
*      Number fo discritizatins
*          NXD 1   Crossing
*          NRD 10  Radial
*
*      Etc
*          PI  3.14i5  Pai
*          AVM 6.022e5 Avogadro's number in this units
*              = 6.022e23 / ( 1e15 * 1e3 )
*                  1e15    1 liter = CL mivro-m^3
*                  1e3     1 M     = CM mM
*
*  Drived constants
*
*      VV  4/3*PI*RV^3     Volume of the vesicle
*      RT  CR*NXD/(WX*AVM) AchR concentration
*      ET  NE/(VC*AVM)     AchE concentration
*      AT  NA/(VV*AVM)     Ach concentaration per MEPC
*      DSS DS*PI*FR*(RP+ER*t)^2/(VV*LP)
*
```

```
 ************************************************************************/
#include    "matrix.h"

#define     AVM     6.022e5
#define     PI      3.1415

#define     NSTATES     81          /* Max Value of (NRD*(4*NXD+4)+1)   */
#define     NCOEFFS     1
#define     NINPUTS     0
#define     NOUTPUTS    3           /* Number of open channels          */

static  Matrix  *Coeffs[NCOEFFS];
#define     K1  mxGetPr(Coeffs[0])[0]
#define     KM1 mxGetPr(Coeffs[0])[1]
#define     K2  mxGetPr(Coeffs[0])[2]
#define     K3  mxGetPr(Coeffs[0])[3]
#define     KR  mxGetPr(Coeffs[0])[4]
#define     KMR mxGetPr(Coeffs[0])[5]
#define     KO  mxGetPr(Coeffs[0])[6]
#define     KC  mxGetPr(Coeffs[0])[7]
#define     DA  mxGetPr(Coeffs[0])[8]
#define     DS  mxGetPr(Coeffs[0])[9]
#define     WX  mxGetPr(Coeffs[0])[10]
#define     RC  mxGetPr(Coeffs[0])[11]
#define     RV  mxGetPr(Coeffs[0])[12]
#define     RP  mxGetPr(Coeffs[0])[13]
#define     ER  mxGetPr(Coeffs[0])[14]
#define     FR  mxGetPr(Coeffs[0])[15]
#define     LP  mxGetPr(Coeffs[0])[16]
#define     VC  mxGetPr(Coeffs[0])[17]
#define     NA  mxGetPr(Coeffs[0])[18]
#define     NE  mxGetPr(Coeffs[0])[19]
#define     CR  mxGetPr(Coeffs[0])[20]
#define     RNXD    mxGetPr(Coeffs[0])[21]
#define     RNRD    mxGetPr(Coeffs[0])[22]

#define     A0(X,R) x0[NRD*(X)+(R)]
#define     B0(X,R) x0[NRD*(NXD+(X))+(R)]
#define     F0(X,R) x0[NRD*(2*NXD+(X))+(R)]
#define     E0(X,R) x0[NRD*(3*NXD+(X))+(R)]
#define     U0(R)   x0[NRD*(4*NXD)+(R)]
#define     V0(R)   x0[NRD*(4*NXD+1)+(R)]
#define     O0(R)   x0[NRD*(4*NXD+2)+(R)]
#define     R0(R)   x0[NRD*(4*NXD+3)+(R)]
#define     S0      x0[NRD*(4*NXD+4)]

#define     BCX(X)  ((X)<0?0:((X)>=NXD?NXD-1:(X)))
#define     BCR(R)  ((R)<0?0:(R))

#define     A(X,R)  ((R)>=NRD?0:x[NRD*BCX(X)+BCR(R)])
#define     B(X,R)  x[NRD*(NXD+(X))+(R)]
#define     F(X,R)  x[NRD*(2*NXD+(X))+(R)]
#define     E(X,R)  x[NRD*(3*NXD+(X))+(R)]
#define     U(R)    x[NRD*(4*NXD)+(R)]
#define     V(R)    x[NRD*(4*NXD+1)+(R)]
#define     O(R)    x[NRD*(4*NXD+2)+(R)]
#define     R(R)    x[NRD*(4*NXD+3)+(R)]
```

```
#define     S       x[NRD*(4*NXD+4)]

#define     dA(X,R) dx[NRD*(X)+(R)]
#define     dB(X,R) dx[NRD*(NXD+(X))+(R)]
#define     dF(X,R) dx[NRD*(2*NXD+(X))+(R)]
#define     dE(X,R) dx[NRD*(3*NXD+(X))+(R)]
#define     dU(R)   dx[NRD*(4*NXD)+(R)]
#define     dV(R)   dx[NRD*(4*NXD+1)+(R)]
#define     dO(R)   dx[NRD*(4*NXD+2)+(R)]
#define     dR(R)   dx[NRD*(4*NXD+3)+(R)]
#define     dS      dx[NRD*(4*NXD+4)]

static  int NXD;
static  int NRD;

static  double  DX2;                    /* DA/(UX*UX)                */
static  double  DR2;                    /* DA/(UR*UR)                */
static  double  DSF;                    /* DS*pi/(VV*LP)             */
static  double  VPV;                    /* Ratio of VV to VS         */
static  double  OCE;        /* Volume of first critical disc unit    */
static  double  AT;

void    init_conditions(x0)
double  *x0;
    {
    double  RT  = CR*RNXD/(WX*AVM);
    double  ET  = NE/(VC*AVM);
    double  VV  = 4./3.*PI*RV*RV*RV;
    double  UX;                         /* Delta x                   */
    double  UR;                         /* Delta r                   */
    double  VS;                         /* Volume of A(0,0)          */
    int i,j;

    AT  = NA/(VV*AVM);
    NXD = RNXD + 0.5;
    NRD = RNRD + 0.5;
    UX  = WX/NXD;
    UR  = RC/NRD;
    DX2 = DA/(UX*UX);
    DR2 = DA/(UR*UR);
    DSF = DS*FR*PI/(VV*LP);
    VS  = PI*UR*UR*UX;
    VPV = VV/VS;
    OCE = VS*AVM;

    for( i = 0; i < NXD; i++ )
        for( j = 0; j < NRD; j++ )
        {
        AO(i,j) = BO(i,j) = FO(i,j) = 0.0;
        EO(i,j) = ET;
        }
    for( j = 0; j < NRD; j++ )
        {
        UO(j) = VO(j) = OO(j) = 0.0;
        RO(j) = RT;
        }
    SO = AT;
```

```
    }

void    derivatives(t,x,u,dx)
    double  t,*x,*u;
    double  *dx;
    {
    double  rop();
    double  f1, f2, f3, f4, f5, f6, f7;
    int i,j;

    for( j = 0; j < NRD; j++ )
        {
        for( i = 0; i < NXD; i++ )
            {
            f1  = - K1*E(i,j)*A(i,j) + KM1*B(i,j);
            f2  = K2*B(i,j);
            f3  = K3*F(i,j);
            dA(i,j) = f1
                + DX2*( A(i-1,j) - 2*A(i,j) + A(i+1,j) )
                + DR2*( A(i,j-1) - 2*A(i,j) + A(i,j+1)
                        + ( A(i,j+1) - A(i,j-1) )/( 2.0*( j + 0.5 ) ) );
            dB(i,j) = - f1 - f2;
            dF(i,j) = f2 - f3;
            dE(i,j) = f1 + f3;
            }
        --i;
        f4  = - 2*KR*A(i,j)*R(j) + KMR*U(j);
        f5  = - KR*A(i,j)*U(j) + 2*KMR*V(j);
        f6  = KO*V(j) - KC*O(j);
        dA(i,j) += f4 + f5;
        dU(j)   = - f4 + f5;
        dV(j)   = - f5 - f6;
        dO(j)   = f6;
        dR(j)   = f4;
        }
    f7 = rop( t );
    dS = DSF*f7*f7*( A(0,0) - S );
    dA(0,0) -= VPV*dS;
    }

double  outputs(t,x,u,y)
double  t,*x,*u;
double  *y;
    {
    double  rop();
    int j;
    double  osum = 0.0;

    for( j = 0; j < NRD; j++ )
        osum += ( 2*j + 1 )*O(j);
    y[0] = osum*OCE;
    y[1] = S/AT;
    y[2] = rop( t );
    }

static  double  rop( t )
double  t;
```

```
    {
    double  rp;
    return( ( rp = RP + ER*t ) < RV ? rp : RV );
    }

#include        "simulink.h"
```

## 3. The procedures of the simulations

The following list defines the functions for the execution of numerical integration in the form of M-files:

- gets_ir: for the execution of the model for the instantaneous release of ACh.
- seti_ir: for the setting of the parameters for the instantaneous release of ACh.
- gets_rm: for the execution of the model for the ACh release mechanisms.
- seti_rm: for the setting of the parameters for the ACh release mechanism.
- plot : for the plotting of $C(t)$.

```
%*********************************************************************
%
% gets_ir: for the execution of the model for the instantaneous
%          release of ACh.
%
%*********************************************************************
function TC = gets_ir(plst)
if ~nargin
    disp(' Usage:   [t,s,Co] = gets([i1 v1 i2 v2 ...])');
    disp('   1: K1   2: KM1  3: K2   4: K3   5: KR');
    disp('   6: KMR  7: KO   8: KC   9: DX  10: DR');
    disp('  11: WX  12: DF  13: RC  14: ST  15: NA');
    disp('  16: NE  17: CR  18: NXD 19: NFD 20: NRD');
    disp('  21: RVN 22: RFN 23: DEN 24: TEND');
    return;
end
global plist dfunc;
DP = seti_ir;
while ~isempty(plst)
    DP(plst(1)) = plst(2);
    plst = plst(3:length(plst));
end
NXD = DP(18);
NFD = DP(19);
NRD = DP(20);
RFN = DP(22);
DEN = DP(23);
plist   = [NXD NFD NRD RFN DEN];
nstates = NRD*NXD*4 + ( NRD - RFN )*4 + RFN*NFD + RFN*DEN*3 + DEN*4;
%Rerr   = 1e-3;
Rerr    = 1e-5;
%Tmin   = DP(24)/500;
Tmin    = DP(24)/1000;
Tmax    = DP(24)/20;
OPT = [Rerr,Tmin,Tmax,0,0,0];
```

```
if isempty(dfunc)
    dfunc = 'diffun';
end
[t,s,Co]= gear(dfunc,DP(24),[],OPT,[],DP(1:23));
TC  = [t,Co,s(:,1:nstates)];


%**********************************************************************
%
% seti_ir: for the setting of the parameters for the instantaneous
%          release of ACh (mM msec micro-m system).
%
%**********************************************************************
function    d = seti_ir

K1  = 200;      % 1
KM1 = 1;        % 2
K2  = 110;      % 3
K3  = 20;       % 4
KR  = 30;       % 5
KMR = 10;       % 6
KO  = 20;       % 7
KC  = 5;        % 8
DX  = 0.1;      % 9
DR  = 0.1;      %10
WX  = 0.05;     %11
DF  = 0.5;      %12
RC  = 0.5;      %13
ST  = 9000;     %14
NA  = 1e4;      %15
NE  = 2e7;      %16
CR  = 2e4;      %17
NXD = 3;        %18
NFD = 30;       %19
NRD = 10;       %20
RVN = 1;        %21
RFN = 1;        %22
DEN = 15;       %23
TEND    = 5.0;      %24

d = [K1,KM1,K2,K3,KR,KMR,KO,KC,DX,DR,WX,DF,RC,ST,NA,NE,CR,...
    NXD,NFD,NRD,RVN,RFN,DEN,TEND];


%**********************************************************************
%
% gets_rm: for the execution of the model for the ACh release
%          mechanism.
%
%**********************************************************************
function TC = gets_rm(plst)
if ~nargin
    disp(' Usage:   [t,s,Co] = gets([i1 v1 i2 v2 ...])');
    disp('   1: K1   2: KM1  3: K2   4: K3   5: KR');
    disp('   6: KMR  7: KO   8: KC   9: DA  10: DS');
    disp('  11: WX  12: RC  13: RV  14: RP  15: ER');
    disp('  16: FR  17: LP  18: VC  19: NA  20: NE');
```

```
    disp('  21: CR  22: NXD 23: NRD 24: TEND');
    return;
end
global t s DP dfunc;
DP = seti_rm;
while ~isempty(plst)
    DP(plst(1)) = plst(2);
    plst = plst(3:length(plst));
end
%Rerr   = 1e-3;
Rerr    = 1e-5;
%Tmin   = DP(24)/500;
Tmin    = DP(24)/1000;
Tmax    = DP(24)/20;
OPT = [Rerr,Tmin,Tmax,0,0,0];
if isempty(dfunc)
    dfunc = 'diffun';
end
[t,s,Co]= gear(dfunc,DP(24),[],OPT,[],DP(1:23));
TC  = [t,Co];


%*********************************************************************
%
% seti_rm: for the setting of the parameters for the ACh release
%          mechanism (mM msec micro-m system).
%
%*********************************************************************
function    d = seti_rm

K1  = 200;      % 1
KM1 = 1;        % 2
K2  = 110;      % 3
K3  = 20;       % 4
KR  = 30;       % 5
KMR = 10;       % 6
KO  = 20;       % 7
KC  = 5;        % 8
DA  = 0.1;      % 9
DS  = 0.1;      %10
WX  = 0.05;     %11
RC  = 0.5;      %12
RV  = 1.85e-2;  %13
RP  = 1.00e-3;  %14
ER  = 2.50e-2;  %15
FR  = 1.0;      %16
LP  = 1.00e-2;  %17
VC  = 450;      %18
NA  = 1e4;      %19
NE  = 2e7;      %20
CR  = 2e4;      %21
NXD = 1;        %22
NRD = 10;       %23
TEND= 7.0;      %24

d = [ K1,KM1,K2,K3,KR,KMR,KO,KC,DA,DS,WX,...
        RC,RV,RP,ER,FR,LP,VC,NA,NE,CR,NXD,NRD,TEND ];
```

```
%*********************************************************************
%
% plot    : for the plotting of C(t)
%
%*********************************************************************
function plot(plst,cn)
color = ['y' 'm' 'c' 'r' 'g' 'b' 'w'];
TC = gets(plst);
plot(TC(:,1),TC(:,2),color(cn));
xlabel('Time (msec)');
ylabel('Open channels/quantum');
```

本学関係